Gas sensing based on organic composite materials: Review of sensor types, Progresses and Challenges

Abdelghaffar Nasri, Mathieu Petrissans, Vanessa Fierro, Alain Celzard

Gas sensing based on organic composite materials:

Review of sensor types, Progresses and Challenges

Abdelghaffar Nasri[1], Mathieu Pétrissans[2], Vanessa Fierro[1] and Alain Celzard[1*]

[1] Université de Lorraine, CNRS, IJL, F-88000 Epinal, France

[2] Université de Lorraine, INRAE, LERMAB, F-88000 Epinal, France

[*] Corresponding author. Tel: + 33 372 74 96 15. Fax: + 33 372 74 96 38. E-mail address : alain.celzard@univ-lorraine.fr (A. Celzard)

Abstract

Over the past decade, organic semiconductors and renewable resources have aroused great interest in basic research and practical applications. Composites based on organic materials and materials of biological origin, if not all bio-based, are potentially abundant and partly biodegradable. These materials have demonstrated advantages making them ideally suited for gas-sensing applications. Herein, we present different detection principles of gas sensing, such as electrochemical, resistive, capacitive, and acoustic sensors. Besides, we describe sensing properties and suitable materials to enhance the selectivity, sensitivity and response/recovery time of gas sensors. In addition, an overview of different forms of materials based on renewable resources and inorganic/organic semiconductors, as well as the development of different types of sensors are discussed. Finally, challenges and future directions are examined in order to develop a low-cost microscale sensing technology using composite materials based on renewable resources. We anticipate that chemical engineering, computer science, machine learning and embedded systems can contribute to the development of new sensing materials.

I. Introduction

Organic semiconductors have attracted the attention of researchers for various applications such as organic light emitting diodes (OLEDs) [1] organic photovoltaic cells [2], supercapacitors [3], organic field-effect transistors (OFETs) [4] and sensors. Organic semiconductors are giving rise to a new generation of electronic devices with low cost and low power consumption, as well as greater flexibility and lightness. In recent years, organic semiconductors have become particularly promising materials for sensors. In particular, graphene and carbon nanotubes (CNTs) are widely known and used for gas sensing applications [5–8].

A sensor is a transducer that induces a measurable output from a known input stimulus, whether physical or chemical. Usually, the output signal is proportional to the input stimulus and this property is used in gas sensors, which are devices that can be used to measure the concentration and/or identify the sensed gas by analysing the reactions between the sensing material and gases or vapours. Gas sensors have many applications such as environmental monitoring [9], medical diagnostics [10], or food quality control [11]. From this perspective, chemical sensors can help monitor the state of human health and, in part, that of the environment [12,13].

The performance of gas sensors can be evaluated through certain parameters, including selectivity, sensitivity, operating temperature, response/recovery time and detection limit. The sensor response, or sensitivity, is generally defined in two forms: S (%) = $[(S_g - S_a) / S_a] \times 100$, or S (dimensionless) = S_g / S_a, where S_a and S_g are the sensor output signals in air and in the target gas, respectively. Obviously, S (%) = S (dimensionless) - 1. The type of signal depends on the type of sensor used (resistive, capacitive, electrochemical, etc.). The sensor is also characterised by its response and recovery times, which are the times required to achieve a 90% change in sensor response when exposed to gas and in the absence of gas, respectively.

The latest technologies such as chemical engineering, machine learning, computer sciences, Internet of Things (IoT), artificial intelligence and communication technologies are improving detection systems. On the one hand, they pave the way for the creation of compact, lightweight and smart systems. On the other hand, they contribute to the manufacture of devices that are more environmentally friendly, consume less energy, and are more stable and less expensive. In addition, these new technologies promote the creation of inexpensive environmental monitoring methods, reduce the cost of the gas sensor's analyser block and accelerate the development of new materials for gas sensing applications.

Advances in materials science are giving rise to a new generation of materials called "hybrid materials" or "mixed materials", here simply referred to as "composite materials", which are based on organic semiconductors and biomass derivatives. These combinations result in advanced materials having in common good electrical conductivity, mechanical strength and thermal stability [14]. In Figure 1, a general approach to the use of cellulose and organic semiconductor to make composite materials of different types to serve various applications is presented. These materials can certainly stimulate future research and lead to economic gains with respect to the moderate costs of raw materials and their processing methods.

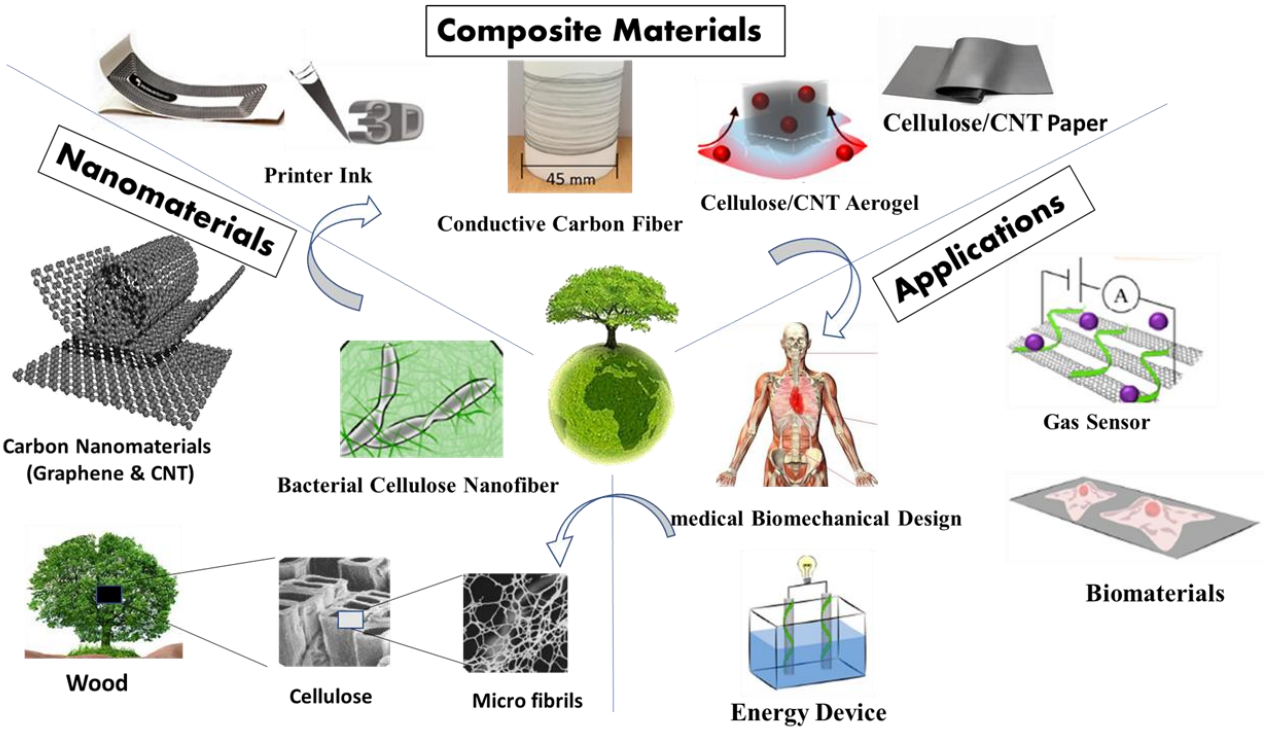

Figure 1. Diagram showing the use of composite materials (here based on cellulose, nanocellulose and CNTs or graphene) for various applications.

As the gas sensing system can have a detection principle based on different types of sensors, it can therefore have different structures. Moreover, depending on the detection method, the output signal can be completely different. Thus, there are different type of sensors such as electrochemical, resistive/capacitive, optical and acoustical, the latter being based on mechanical detection structures and micromechanical systems (MEMS). For example, OFETs are generally used for resistive and electrochemical sensors, while metal oxides are used in capacitive sensors. The resistive type is widely used to measure gas concentration in air. The presence of gas can thus change the electrical conductivity of the sensing material, which in turn changes the resistance of the sensing layer as an output signal. In a capacitive system, it is the capacitance of the gas sensor that changes, typically in the order of a few pF, by changing the dielectric constant of the sensing material between two electrodes when the target gas is present. In addition, interdigitated electrodes

(IDEs) structures with a sensing layer can be used for several types of sensors, such as those based on capacitive, resistive, electrochemical and surface acoustic wave (SAW).

To place our work in the context of the state of the art, it should be noted that various previous review articles have investigated the different operating principles of gas sensors [15,16] while others have been conducted on the influence of materials implemented with a single technique [1,17]. But in the present review, we will give a general overview of the different types of sensors with the effects of different materials on their performance.

This review thus discusses different sensors that measure the concentrations of species in the gas phase using various composites based on organic materials. The first part will discuss the different operating principles of gas sensors and the effect of inorganic/organic materials and renewable resources to improve their sensing performance at room temperature. We will present an overview of renewable resource considerations that can be used in a plethora of applications and also to develop a new gas sensor based on 100% renewable resources at a low cost. We will also give some manufacturing techniques for the development of composite materials, and we will present the characteristics and forms of some of them, based on organic semiconductors and cellulose. In addition, we will discuss the challenges, critical issues, future prospects and future research avenues in the field of gas detection. Finally, basic technologies to improve detection performance and environmental monitoring will be described.

II. Types of gas sensors

As this review focuses solely on composites based on organic, and as far as possible renewable, materials, only 4 types of sensors will be considered: electrochemical, resistive, capacitive, and surface acoustic wave sensors. There are of course many other types of gas sensors, but they will not be dealt with here since their mode of operation is incompatible

with the type of materials considered, in particular a too high temperature. Moreover, the operating conditions and responses of the sensors treated here will only be considered at room temperature.

1. Electrochemical sensors

Electrochemical sensors first appeared in the early 1950s to monitor the amount of oxygen in the environment [18]. In the 1980s, these sensors underwent an intense miniaturization process that allowed them to begin to penetrate the market and become capable of detecting many different toxic gases [18]. Today, a large number of electrochemical sensors are widely used in many stationary and portable applications for environmental quality control and human health [19,20].

Electrochemical sensors can be of different types: potentiometric, voltammetric, and amperometric [21]. The amperometric sensor is the most commonly used, and is the one discussed in this section. This type of electrochemical sensor is based on a redox reaction, whereby the target gas reacts in the core of the device comprising an electrolyte and two or three electrodes having catalytic properties. Figure 2.a shows a typical configuration that consists of a sensing electrode (or working electrode), a reference electrode, a counter electrode separated by a thin layer of electrolyte, and a hydrophobic membrane (also called permeable membrane). Sometimes, the membrane is installed in the sensor to filter out unwanted gases but it is also used to cover the sensor's sensing electrode and to monitor the amount of gas molecules reaching the electrode surface. The gas reacts on the surface of the sensing electrode (anode) by an oxidation mechanism. For example, the sensing electrode provides electrons for the oxygen reduction at the cathode. The electrolyte inside the sensor allows the passage of the ionic charge from one electrode to the other. These reactions vary according to the nature of the gas to be measured and, therefore, the choice of the type of material that constitutes the electrode is crucial for the sensitivity of the sensor.

Electrodes with catalytic properties are used in electrochemical sensors to detect common gaseous pollutants. These electrodes return a linear current response as a function of gas concentration [9,22] . To improve the properties of gas sensors, noble metal electrodes are often used and give excellent results [23–25].

Some sensors also require the application of an adjustable but constant voltage to the anode to monitor the selectivity of the gas sensor, making the sensor specific to the target gas by promoting the desired redox reactions [26]. In reality, the potential of the anode does not remain constant due to the electrochemical reaction with gas. If this voltage varies or is absent, the sensor may be unusable and its performance may deteriorate. For this purpose, a reference electrode is placed in the electrolyte, close to the anode, as shown in Figure 2.a. This electrode maintains constant sensitivity, high linearity and increased sensitivity to the target gas. No current flows to or from the reference electrode. The current flow between the anode and the counter-electrode (cathode) is measured and is usually directly related to the gas concentration.

Moreover, there are also sensors known as micro fuel cell electrochemical sensors that do not require a reference electrode (i.e., operate without an external supply voltage). This type can be used as a CO sensor. For example, when CO reaches the anode, CO reacts with water vapour (H_2O) from the air over the catalyst of the electrode, generating carbon dioxide (CO_2) as well as hydrogen ions (H^+) and electrons. During oxidation, electrons are released and then transferred by an external circuit to the cathode to create a current. The hydrogen ions (H^+) generated on the anode pass through the electrolyte, and react with oxygen (O_2) from the air and electrons (e^-) at the cathode, generating water (H_2O).

Electrochemical sensors require a certain amount of oxygen to operate. For example, the electrons released by the oxidation of different common gases through the following reactions:

$$CO + H_2O \rightarrow CO_2 + 2H^+ + 2e^- \quad (1)$$

$$H_2S + 4H_2O \rightarrow H_2SO_4 + 8H^+ + 8e^- \quad (2)$$

$$H_2 \rightarrow 2H^+ + 2e^- \quad (3)$$

$$NO + 2H_2O \rightarrow HNO_3 + 3H^+ + 3e^- \quad (4)$$

are used for the oxygen reduction reaction at the cathode according to:

$$O_2 + 4H^+ + 4e^- \rightarrow 2H_2O \quad (5)$$

For this reason, the presence of oxygen is essential for operation and if its quantity is less than necessary, the sensor may gradually deteriorate.

The electrode material, sensing material and the structure of the sensor have an impact on the performance of the gas sensor [21,27,28]. Some structures of organic electrochemical sensors are presented in Figure 2.

In sensor applications, organic materials have been used as the sensing layer because they are sensitive to a range of stimuli, including pH value, and the presence of gas molecules or biomolecules. Organic semiconductors have unique mechanical and electronic properties suitable for the development of low-cost devices. Moreover, these materials can exhibit excellent electrocatalytic activity with respect to redox behaviour, such as CNTs, and therefore have good detection performance. In addition, the sensitivity of pure graphene can be improved by mixing it with other materials. For example, to improve carrier diffusion and the adsorption of gas molecules on the surface, graphene can be chemically doped [29]. Alternatively, polyaniline (PANI) has been used to manufacture electrochemical gas sensors using different techniques such as spraying, drop-casting, inkjet printing (IJP) and spin-coating [30–33].

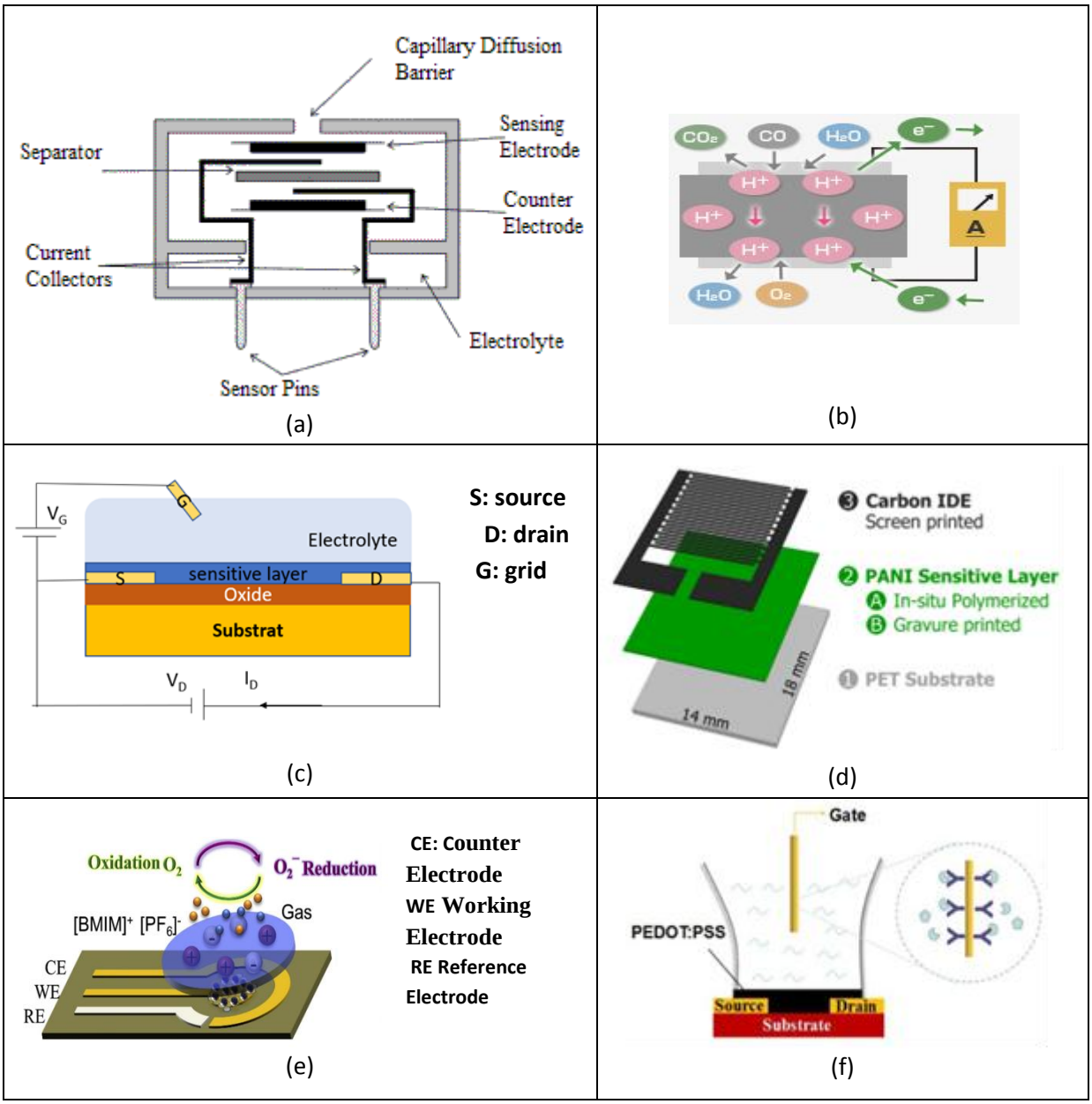

Figure 2. Examples of organic electrochemical device structures based on organic materials: (a) internal structure of an electrochemical gas sensor cell [34] Copyright from the official website of SGX Sensortech; (b) micro fuel cell type electrochemical sensor [35] Copyright From the official website of the Figaro Engineering Inc; (c) typical organic electrochemical transistor (OECT) sensor; (d) sensor structure with layers ordering (the polyaniline (PANI) layer was either in-situ polymerised or printed) [36]. Copyright Sensors and Actuators B: Chemical; (e) Graphene oxide and carbon-gold nanocomposite ionic liquid-based electrochemical gas sensor [37] Copyright Sensors and Actuators B: Chemical; (f) OFET biological sensor structure based on Poly (3,4-ethylenedioxythiophene) doped with polystyrene sulfonate (PEDOT: PSS) [38] Copyright MDPI Sensors.

Thus, Syrový et al. [36] investigated the effect of the variation in the gap of Interdigitated Electrodes (IDEs) on the performance of an electrochemical gas sensor produced by the IJP

technique. The structure of the gas sensor consists of two carbon IDEs and PANI as a sensing layer on a polyethylene terephthalate (PET) substrate, as shown in Figure 2.d [36]. The authors used novel colloids of polyaniline hydrochloride, which were synthesised in xylene or chloroform in the presence of a surfactant, as a printing formulation. They presented the sensor characteristics of colloid-based sensitive layers and compared them with those of in-situ polymerised polyaniline layers. The colloid-based sensors have shown better sensing performance at low ammonia concentration [36].

In addition, various researchers have studied electrochemical sensors based on organic field effect transistors (OFETs) and thin film transistors (TFTs). Thus, Kumar et al. demonstrated the applicability of an OFET based on Poly [N- 90 -heptadecanyl-2, 7-carbazole-alt-5, 5-(40, 70 -di-2- thienyl-20, 10, 30 -benzothiadiazole] (PCDTBT) for the detection of NO_2 gas at the ppm level. The electron removal from the NO_2 molecule by the p–type semiconducting polymer PCDTBT resulted in an increase in conductivity. For a dose of 2 ppm NO_2 at gate bias of -10 V, the sensor exhibited typical response and recovery times values equal to 16.2 s and 171 s, respectively [39].

Besides, Wan et al. [37] presented an electrochemical gas sensor based on carbon-gold nanocomposites (GCN) on reduced graphene oxide (rGO) [37]. The authors used a hydrothermal technique to synthesise the CGN by carbonisation of glucose and deposition of gold nanoparticles. The rGO was then electrochemically deposited on a screen-printed gold electrode, with subsequent modification of the CGNs. Figure 2.e shows the modified rGO-CGN electrochemical gas sensor. In order to improve the stability and lifetime of the sensor, Wan et al. used a thin-film ionic liquid electrolyte. The sensor was set to detect 0.42% to 21% oxygen, and showed good linearity and high sensitivity [37].

Further on, organic electrochemical transistors can be used for biological detection. Poly (3,4-ethylenedioxythiophene) doped with polystyrene sulfonate (PEDOT:PSS) has achieved

excellent results for bioelectronic applications. PEDOT:PSS-based OFETs have been successfully used to detect human influenza virus [40], bacteria E. coli O157:H7 [41] and glucose [42]. Figure.2.f shows a biosensor device based on PEDOT:PSS, whose structure consisted of a channel composed of PEDOT: PSS between the source (S) and the drain (D). The third electrode, called grid, was separated from the channel by an electrolyte.

2. Resistive sensors

The resistive type of sensor is based on the change in conductivity by the presence of adsorbed gas molecules. The response of the sensor is therefore dependent on the interactions between the target gas and the surface, as well as the area available for adsorption and desorption. For example, in the case of gas sensors with an n-type detection layer, when air comes into contact, oxygen is adsorbed as oxide ions after capturing electrons on the surface of the sensing layer surface.

Therefore, when certain reducing (or oxidising) vapour interacts with the sensing layer, the gas molecules (donor or acceptor) interact with these adsorbed oxygen ions, thus decreasing (or increasing) the electron density in the conduction band. As a result, the resistance of the gas sensor increases (or decreases) relatively [43,44]. In case of a p-type sensing layer, the reciprocal phenomenon occurs [45]. Table 1 summarises the detection mechanisms of resistive sensors.

Table 1. Detection mechanisms and corresponding changes of electrical resistance

Conductivity type	Effect of the reducing gas (donor)	Effect of the oxidising gas (acceptor)
n	Decrease of resistance	Increase of resistance
p	Increase of resistance	Decrease of resistance

For example, experimental results show that electron donors such as carbon monoxide (CO) and ammonia (NH_3) tend to decrease electron density, and consequently the resistance of the sensor increases. Conversely, the resistance decreases for electron acceptors such as nitrogen dioxide (NO_2) and water vapour (H_2O).

Metal oxides and organic semiconductors play an important role in improving sensor performance. This is made possible by optimising various parameters such as composition, synthesis methods, morphology and structure. Different metal oxide semiconductors (such as WO_3, SnO_2, ZnO, TiO_2) are easily combined with various organic semiconductors such as graphene, single-walled or multi-walled carbon nanotubes (SWCNTs and MWCNTs, respectively), and zinc oxide (ZnO) with graphene oxide nanoribbons (GONR) (ZnO/GONR). The impact of different structures based on these materials, at room temperature, will be discussed in the following paragraphs.

For example, Wang et al. [46] found that the addition of ZnO nanoparticles to GONR improves selectivity of toluene gas sensor [46]. The ZnO/GONR-based sensor has better sensitivity and shorter response/recovery time than the pure ZnO-based sensor, as shown in Table 2. Seekaew et al. [47] studied a toluene gas sensor based on 3D titanium dioxide/graphene-carbon nanotubes (3D TiO_2/G-CNT) fabricated by Chemical Vapour Deposition and sparking methods. The corresponding sensor stucture is shown in Figure 3.a. The sensing performance as a response to 500 ppm toluene vapor was compared to that of other related carbon nanostructures. The gas responses of CNTs, graphene, TiO_2-CNT, 3D G-CNT and 3D TiO_2/G-CNT sensors were about 1.5%, 1.9% , 2.8%, 6.9% and 42.9%, respectively. The 3D TiO_2/G-CNT gas sensor thus showed the highest response for toluene.

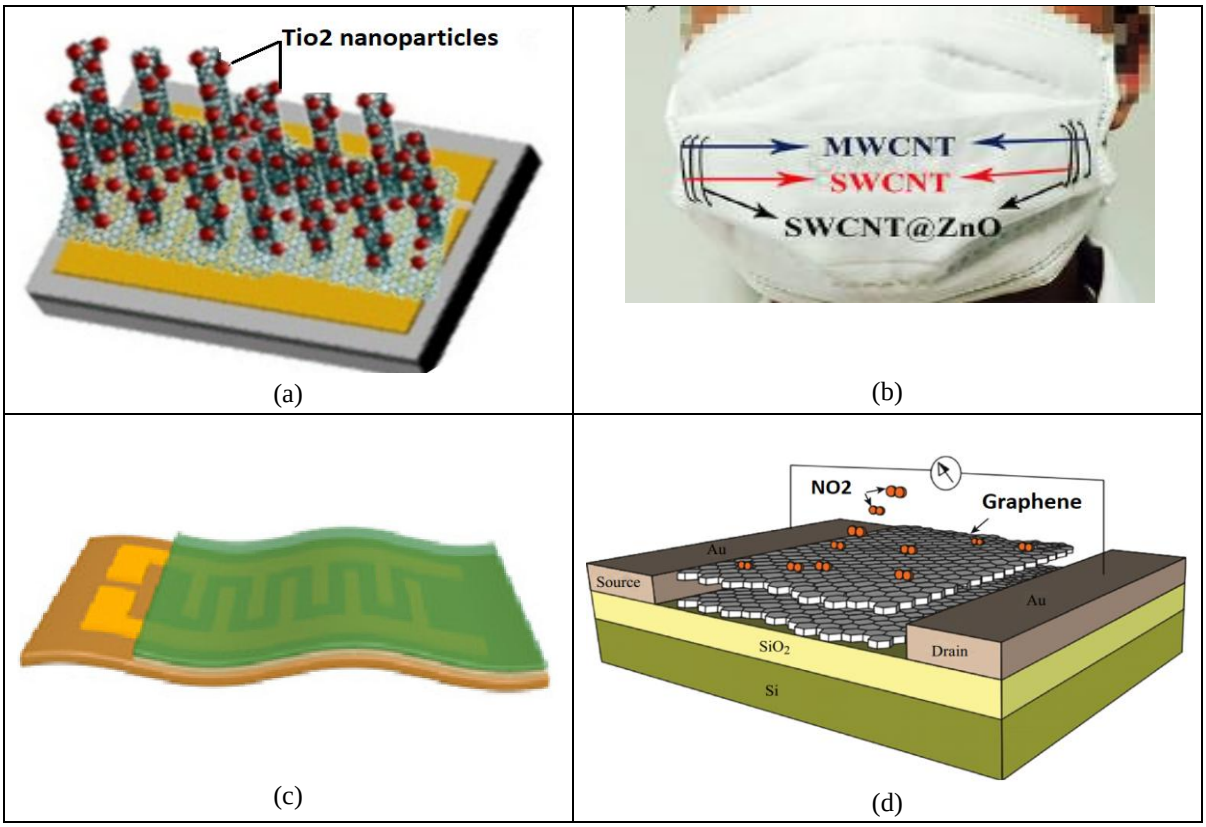

Figure 3. Examples of structures of resistive gas sensors made from various materials and having different structures: (a) 3D nanostructured TiO_2/G-CNT gas sensor [47] (b); fibrous gas sensor based on MWCNTs, SWCNTs, and SWCNTs@ZnO integrated into a smart face mask [48]; (c) structure of a gas sensor based on PPy/N-MWCNT with flexible polyimide substrate and IDEs [49]; (d) graphene-based OFET as gas sensor [50].

In 2018, Gao et al. [48] have manufactured flexible fibrous gas sensors based on MWCNTs, SWCNTs and SWCNTs decorated with ZnO quantum dots (ZnO/SWCNTs). These fibres have been integrated into nylon-based portable smart masks, as shown in Figure 3.b. The influence of the sensing materials on sensitivity and recovery times was investigated for different gases (Table 2). At a concentration of 500 ppm, sensors based on SWCNTs, MWCNTs and ZnO/SWCNTs were used to detect ammonia, formaldehyde and ethanol vapour, respectively. As a result, the sensitivity responses obtained were 11, 18 and 9%, respectively. In addition, the sensors showed good response (and recovery) times equal to 1004 s (1005 s) for SWCNTs, 798 s (464 s) for MWCNTs and 992 s (301 s) for ZnO/SWCNTs (see Table 2).

In addition, the fibers could be used as conducting wires; each sensor was connected to an independent red, green or blue light-emitting diode (LED). The reading of the different colours of the LEDs was used to identify ammonia (NH_3), formaldehyde (HCHO) or ethanol (C_2H_5OH). For example, in the case of NH_3, all the three sensors had a sensing response, all LEDs were lit. With the elimination of the NH_3 gas, the resistances of the three gas sensors returned to their initial values, turning off all three LEDs. In the case of HCHO gas, only SWCNTs and ZnO/SWCNT reacted, and the green and blue LEDs lit. Ethanol only affected the resistance of the ZnO/SWCNT sensor, so the blue LED illuminated when this gas was introduced [48].

Resistive sensors have been extensively studied for the detection and quantification of nitrogen dioxide (NO_2) gas, based on different materials and under different structures, and have shown satisfactory results as can be seen in Table 2. The combination of different materials has led to improved NO_2 detection properties, for example using: SnO_2 nanocrystals-decorated MWCNTs with IDEs structure [51], molybdenum disulfide (MoS_2)/graphene hybrid aerogel [52], polypyrrole/nitrogen-doped MWCNTs (PPy/N-MWCNT) on polyimide (PI) as flexible substrate [49], SWCNT/PPy spin-coated onto pre-patterned electrodes [53], and ZnO/GONR deposited onto a GaN substrate [46].

IDEs with a sensing material deposited on a substrate are also used for the application of resistive gas sensors. For example, the composite PPy/N-MWCNT stucture on a flexible polyimide substrate and IDEs, as shown in Figure 3.c, has been successfully prepared using a combined in situ self-assembly and annealing treatment method. The structure was tested in a NO_2 concentration range from 1 to 50 ppm. Liu et al. [49] showed that the annealing treatment plays an important role in improving detection properties. For example, the response of the optimal material was 44.12 times greater than that of an unannealed one, whereas the relative response was 24.82% at low concentration of 5 ppm NO_2 (see Table 2).

Response and recovery times were 65 s and 668 s, respectively. In another example, polypyrrole nanoparticles (PPyNPs) were used to improve the response of an ammonia sensor based on IDEs by Kim et al. [54]. Good sensitivity (2.5%) was obtained, with short response and recovery times, at low ammonia concentration (down to 1 ppb of NH_3).

Wei et al [55] studied the influence of the geometric structure of the IDEs (line width / gap width, see numerical values in Table 2) on the response of ethanol and methane gas sensors. The sensing material had been developed with a mixture of polyvinylpyrrolidone (PNVP), carbon black and ethylene glycol, which was then applied on the IDEs. It was deduced that the sensitivity of the gas sensor is inversely proportional to the gap of the electrodes.

In addition, the OFET structure is also used for resistive gas sensors based on different organic materials. Figure 3.d shows an example of the OFET structure of a graphene-based NO_2 sensor [50].

It is worth noticing that a given sensing material may give different sensing performance, depending on the bibliographic reference. Indeed, not only the nature of the sensing material has an influence on the response of the sensor, but many other parameters may also play an important role. These are, for instance, the overall structure of the device, the nature of the substrate, the existence of other phases present, the surface quality, some defects in the sensing layer, the level of doping, etc. Thus, as seen in Table 2, the same ZnO: SWCNT sensing material gave different sensitivities to the same gas. This is because either a flexible fibrous gas sensor based on ZnO: SWCNT integrated in nylon-based portable smart masks has been used [48], or a thin film ZnO: SWCNT gas sensor obtained by painting a powder-based paste on an alumina substrate has been produced [56].

In summary, different structures can be used for resistive gas sensors. Decorating organic semiconductors with an oxide can improve selectivity and sensitivity. The decorating oxide

used depends on the target gas. In addition, the dimensionality (0, 1, 2 or 3D) of the sensing material and the area available for adsorption can also improve sensor performance. Examples of performance at room temperature of resistive gas sensors with different structures and made from different materials are shown in Table 2.

Table 2. Performance of some examples of resistive gas sensors with different structures and made from different materials at room temperature.

Sensing materials	Sensitivity	Gas	Concentration (ppm)	Response time (s)	Recovery time (s)	References
3D TiO_2 /G-CNT	42%	Toluene vapour, C_7H_8	500	10	11	[47]
3D G-CNT	6.3%		500	8	9	
PPy/NMWCNT	24.82%	Nitrogen dioxide, NO_2	under 5	65	668	[49]
SWCNT/PPy	25% 6%		3000 200	3000	5400	[53]
SWCNT	11%	Formaldehyde, HCHO	500	1004	1005	[48]
ZnO : SWCNT	9%	Ethanol, C_2H_5OH	500	992	301	
MWCNT	18%	Ammonia, NH_3	500	798	464	
ZnO : SWCNT	300%	Ethanol, C_2H_5OH	300	300	100–150	[56]
ZnO/GONR	1675%	Nitrogen dioxide, NO_2	50	31	27	[46]
ZnO	675%		50	130	133	
PPyNPs	2.5%	Ammonia, NH_3	0.1	19	49	[54]
PNVP 20 μm/20 μm 50 μm/75 μm	 7.5 % 2.3 %	Ethanol, C_2H_5OH	 800	60 150	180 450	[55]
PNVP 20 μm/20 μm 40 μm/60 μm	 8 % 4.5 %	Methane, CH_4	160	900 500	100 1000	[55]
SnO_2-NC/ MWCNTs	180%	Nitrogen dioxide, NO_2	100 ppm	580	620 s	[51]
MoS_2/Graphene hybrid aerogel	10%	Nitrogen dioxide, NO_2	0.5	420	650	[52]

From the point of view of manufacturing cost and performance of the different structures used for a resistive sensor, the IDE structure is the one that gives satisfactory results at a lower cost. Furthermore, this structure is the most suitable for use as a biodegradable sensor. In addition, with the IDE structure, a large interaction area is obtained between the electrodes and the sensitive layer, which can improve the performance of the sensor. It can also be used for a capacitive sensor.

3. Capacitive sensors

The capacitive measurement technology involves an AC input, where frequency is an additional input parameter, and measures the change in capacitance due to the change in the effective dielectric constant ($\varepsilon_{r\ eff}$) when the sensor is exposed to gas [57]. The capacitance depends on the effective dielectric constant ($\varepsilon_{r\ eff}$), the electrode area (A) and the thickness of the dielectric layer (d), and is expressed by Eq. (6):

$$C = \frac{\varepsilon_0 \varepsilon_{r\ eff} A}{d} \tag{6}$$

where (ε_0) is the permittivity of vacuum.

Impedance spectroscopy can also be used to analyse the impedance of the sensor as a function of frequency in the presence of a gas. Frequency analysis helps to find the equivalent circuit of the structure and also provides information on the resonance frequency. Using the Cole-Cole diagram (imaginary part of the impedance vs. real part of the impedance), the elements of the equivalent circuit can be derived quantitatively, allowing the physical phenomenon occurring in the nanostructure to be correlated with its interactions with the gas [57,58] The resonance frequency is determined when the minimum imaginary impedance is reached and it plays an important role in defining the selectivity of gas species.

In general, two main structures are used for capacitive sensors such as parallel plate (PP) and IDEs configurations (Figure 4). The impact of different factors such as the sensing

material used, the configuration of the structure, the relative humidity and the thickness of the sensing material, will be discussed in the following paragraphs.

Chen et al. [59] used the PP configuration with arrays of CNTs vertically aligned between two electrodes to detect ammonia (NH_3) and formic acid (HCOOH). The CNT-based gas sensor exhibited good response and recovery times, as shown in Table 3. Vizcaino et al. [60] demonstrated that HCOOH has a higher polarizability and dipole moment than NH_3, resulting in higher intermolecular forces between HCOOH and CNTs. As a result, HCOOH gives a higher detection limit than NH_3, as shown in Table 3.

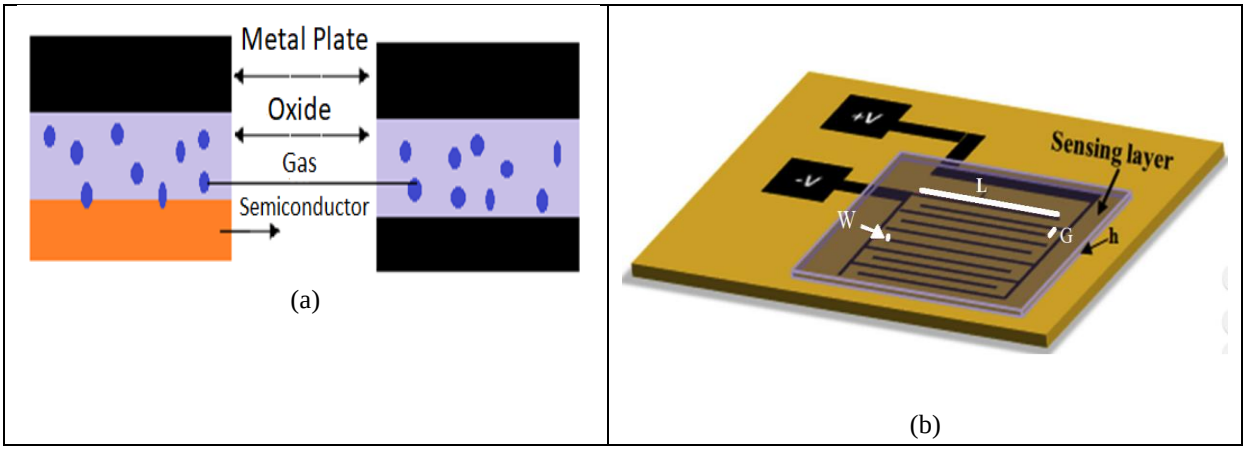

Figure 4. Basic structures for capacitive sensing: (a) PP configuration of Metal Oxide Semiconductor (MOS) (left) or Metal Oxide Metal (MOM) structure (right); (b) IDEs configuration, showing electrode width (W) and length (L), gap (G) between the electrodes, and thickness of the sensing layer (h) [61] with permission from Elsevier.

The IDE configuration has been coated with different materials to detect different gases. Andrés et al. [62] used a structure based on gold IDEs as a capacitive methanol sensor based on MIL-96(Al) Metal Organic Framework (MOF) thin films on a Si/SiO_2 substrate. In another example, the IDE structure was coated with a nano-composite material based on cobalt ferrite ($CoFe_2O_4$), providing a good gas sensor with high sensitivity, dynamic range and selectivity for ethanol gas, even at a very low gas concentration of 7 ppm [63].

A nanocomposite sensing layer, composed of polypyrrole (PPy) and bromoaluminum phthalocyanine (BrAlPc), has been deposited on an IDE structure on a glass substrate. This

sensor offered interesting detection performance, including a sensitivity of 85% to 100 ppm H_2S gas, and short response and recovery times [64]. More details are given in Table 3.

Filippidou et al. [61] used the IDE configuration (see Figure 4.b) based on different polymers such as poly (2-hydroxyethyl methacrylate) (PHEMA), epoxy novolac resin (EPN), poly (methyl methacrylate) (PMMA) and poly (hydroxy styrene) (PHS). The different sensor configurations produced were evaluated when exposed to water, methanol and ethanol vapours. The PHS sensor gave the best response, in particular, by exhibiting capacitance variations ΔC of 44 fF, 7.4 fF and 4.6 fF at 10 000 ppm or each vapour, respectively (see Table 3). Using a definition of sensor sensitivity indicated in certain works such as $S = \Delta C/\text{RH\%}$, where RH% is the relative humidity, the PHS sensor sensitivity for water vapour was 1.87 fF per percent of relative humidity [61].

MWCNTs have been used by Meng et al. [65] to improve the sensitivity in capacitive gas detection. Their sensor structure (Au/Si-SiO_2/Au-MWCNTs) consists of a Si substrate and SiO_2 layer, a gold (Au) layer on the lower surface of the substrate, and Au/MWCNTs electrodes on the upper surface of the structure [65]. Here, the Au electrode was fabricated by screen-printing technique on top of the silicon oxide layer, and MWCNTs were directly grown by CVD. Compared to the effect of spray-casting MWCNTs, the relative capacitance change of the above-mentioned electronic chip was found to increase from 1.8 to 70 in the case of ammonia. MWCNTs modify the contact barrier and improve the gas detection properties for formaldehyde, toluene and ammonia (see Table 3). Graphene oxide-based composite materials [66] have also proved excellent for water detection, as shown in Table 3.

Table 3. Comparative studies between different capacitive gas sensor structures and materials at room temperature.

Sensing materials	Sensitivity = $\left[\frac{\Delta C}{C_0}\right] \times$	Gas or vapour	Concentration (ppm)	Response time (s)	Recovery time (s)	Ref

	100(%), or ΔC (pF)					
CNT	10% 15%	Ammonia, NH_3 Formic acid, HCOOH	15 175	100 20	150 70	[59]
IDEs / PHS	ΔC=44 fF ΔC=4.6 fF ΔC=7.4 fF	Water, H_2O Ethanol, C_2H_5OH Methanol, CH_3OH	10 000	-	-	[61]
Au/Si-SiO2/Au-MWCNTs	3.5% 3.2% 6.8%	Formaldehyde, CH_2 O Toluene, C_7 H_8 Ammonia, NH_3	15 377 155	-	-	[65]
Al/VTP/Al 60 nm 80 nm 90 nm	9.2pF/%RH 7.70pF/%RH 2.55pF/%RH	Water, H_2O	-	15 15 15	10 15 25	[67]
Cu-BTC IDEs/ PP	0.36pF/21pF 0.0 pF/0.0pF -0.15pF/-5.4 pF	Acetone, C_3H_6O Dichloromethane, CH_2Cl_2 Toluene, C_7 H_8	1500	60 / 120 -/- 123 / 60	120 / 150 -/- 120 / 180	[68]
IDEs /MIL-96(Al) MOF	0.088 %	Methanol CH_3OH	2000 (@ 20%RH)	210	-	[62]
Graphene oxide	37 800%	Water, H_2O	From 23%RH to 86%RH	10.5	41	[66]
PPy/ BrAlPc	85%	Hydrogen sulphide, H_2S	100	14	< 14	[64]
IDEs/$CoFe_2O_4$	1000%	Ethanol, C_2H_5OH	100	180	180	[63]

Roslan et al. [67] used the PP configuration based on a VTP phthalocyanine derivative (Vanadyl 3, 10, 17, 24 - Tetra-tert-butyl-1, 8, 15, 22-tetrakis(dimethylamino)-29H, 31H - Phthalocyanine) between two aluminium electrodes on a glass substrate as an organic humidity sensor. The spin coating technique was used to create a PVT layer of controllable thickness (approximately 66, 80 and 90 nm). As shown in Table 3, the thinnest active layer film had the highest sensitivity and shortest recovery time [67].

The PP configuration was compared to the IDEs configuration in the case of capacitive sensors based on nanoparticles of copper-benzene-1, 3, 5-tricarboxylate (Cu-BTC) by Zeinali et al. [68]. Both configurations were used to detect acetone, toluene and dichloromethane at atmospheric pressure, 10% relative humidity and room temperature. The detection performance of these two configurations is shown in Table 3 and demonstrated good linearity and sensitivity. The capacitance behavior showed either an increase or decrease or even no change in the capacity values, as shown in Table 3, depending on the configuration tested. For example, acetone and toluene showed an increase and decrease in capacitance value, respectively. The response to dichloromethane vapour did not change at different concentrations. This different detection behavior depends on the value of the dielectric constant of the absorbed analytes with respect to the dielectric constant of the detection layer. Therefore, it can distinguish between analytes with different dielectric constants [68].

In summary, the IDEs configuration capacitive sensor provided higher detection limit values, shorter recovery time, better repeatability and higher reproducibility than the PP configuration. However, the latter has better sensitivity than the IDEs configuration. In addition, the detection properties can be adjusted not only by using the appropriate sensing layer, but also by selecting the desired IDE geometry (width, number of fingers, spacing, electrode material) and the thickness of the detection layer.

4. Surface acoustic wave sensors

Surface acoustic waves (SAWs) were discovered in 1885 by Lord Rayleigh, and as their name suggests, they are acoustic waves propagating on the surface of a material [69]. SAW sensors have become increasingly popular in recent years due to the increasing miniaturisation of electronic devices. In addition, a SAW sensor can provide a "lab-on-a-chip" type structure with a resolution of a few parts per trillion (ppt). The basic configuration of a SAW sensor consists of two InterDigital Transducers (IDTs) on a piezoelectric substrate.

SAW sensors are based on the principle of the piezoelectric effect. The sensor is remotely interrogated by an electromagnetic wave. This signal is converted into an acoustic wave by the IDTs on the surface of a piezoelectric material. Changes in the physical quantities determining the environment in which the sensor is located (temperature, pressure, chemical composition, etc.) influence the physical properties of the acoustic wave propagating on the sensor surface. In return, the modified wave is transformed into an electromagnetic wave that is sent back to the interrogation unit. The principle of gas detection by microwave transduction is based on the phenomena of propagation and reflection of an incident electromagnetic wave in a sensitive material at frequencies ranging from 300 MHz to 300 GHz.

The characteristics of the reflected and transmitted electromagnetic waves: phase and modulus, depend on the physical and chemical properties of the materials encountered, the interactions with the gas molecules changing their permittivity and modifying the velocity of the electromagnetic waves [70]. Thus, gas-sensitive interactions cause a change in the reflection coefficient, a change in frequency (phase) or an attenuation (amplitude) of the incident electromagnetic waves [71]. The structure and principle of operation of a SAW sensor are presented in Figure 5.a [72].

The permittivity of materials, ε, is a complex quantity dependent on the materials dielectric polarisation in an applied electric field. Since there is a time lag between changes in the alternating electric field and the materials polarisation [73], the frequency of the electric field influences the permittivity of the materials. The latter follows the Maxwell-Garnett equation [74], given by Eq. (7):

$$\varepsilon - \varepsilon_\infty = \varepsilon' - j\varepsilon'' = \frac{\varepsilon_S - \varepsilon_\infty}{1+\omega^2\tau^2} - j\left(\frac{\omega\tau(\varepsilon_S - \varepsilon_\infty)}{1+\omega^2\tau^2} + \frac{\sigma}{\omega\varepsilon_0}\right) \quad (7)$$

where ε_∞ is the permittivity at the high-frequency limit, ε_s is the static permittivity, ω is the angular frequency, σ is the conductivity of the material, ε_0 is the permittivity of vacuum, and τ is the characteristic relaxation time. The imaginary part of the permittivity (ε'') is related to the conductivity of the material, while the real part of the permittivity (ε') is related to the amount of energy from an external electric field that will be stored by the material. Eq. (7) thus explains the origin of the changes in amplitude and frequency.

Many theoretical models for SAW gas sensors have been proposed in the literature. The basic model for presenting the relationship between the output of SAW sensors and the amount of gas absorbed on the sensor surface is mainly that of Wohljent [75]. In 2014, Liu and Lu proposed a new theoretical model by combining the Wohljent approach with the Brunauer-Emmett-Teller (BET) formula. The theoretical model fits well with the experimental data obtained from a commercial SAW gas sensor to detect DiMethyl MethylPhosphonate (DMMP) [76]. Moreover, based on perturbation theory [77], Qi et al. [78] used the COMSOL simulator to present the response of the ZnO-based SAW gas sensor. An experiment was carried out using a SAW gas sensor coated by ZnO to confirm the simulation model.

Many geometric structures are used for microwave gas detection, such as microstrip line, coplanar waveguide, coaxial line and resonant cavity. Examples of sensing materials, propagation structures and response signals used for microwave gas sensors are shown in Table 4.

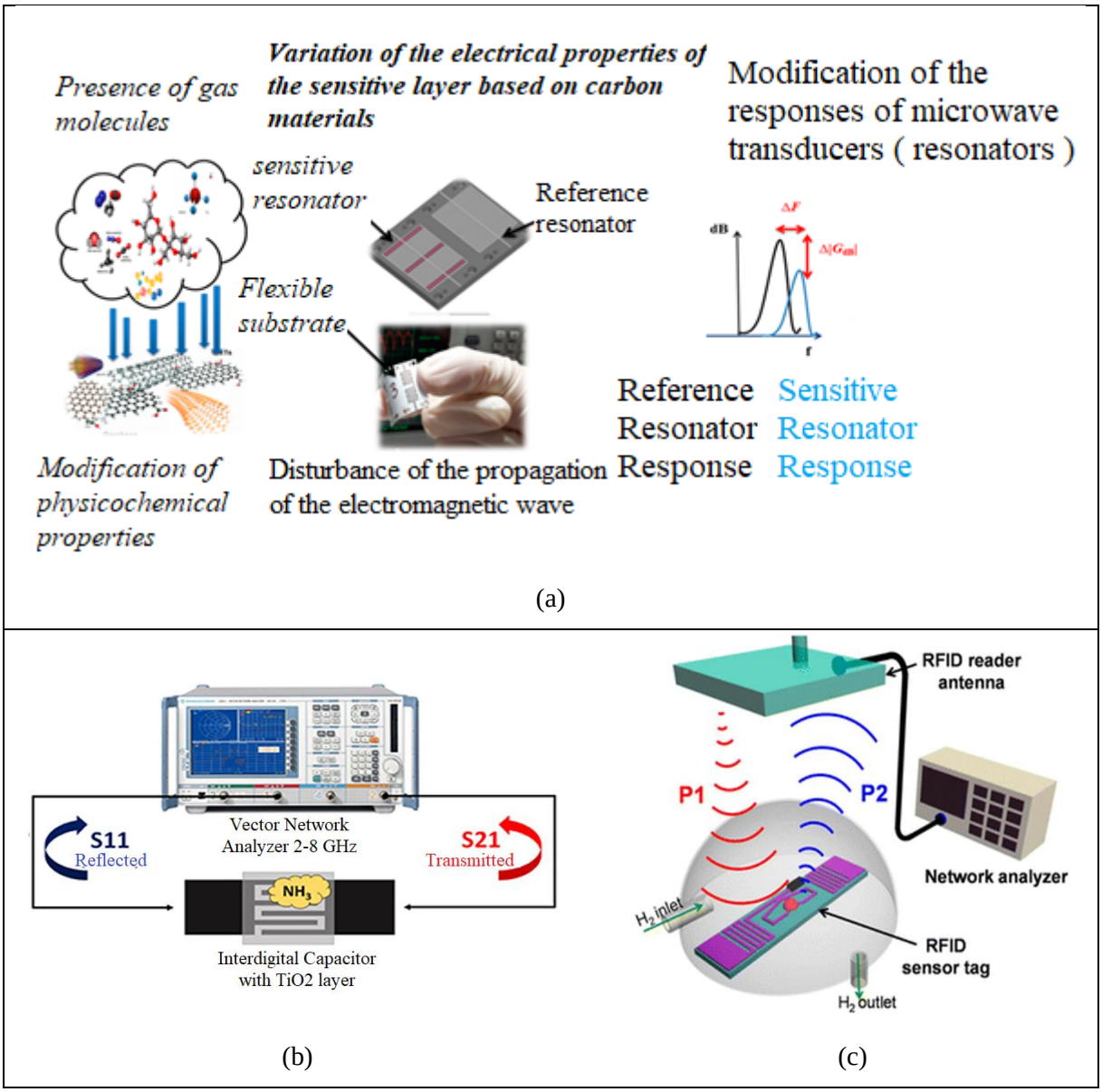

Figure 5. (a) Overview of the operating principle of the SAW sensor [72] Copyright MDPI sensors; (b) Principle of microwave transduction applied to reflection/transmission measurements [79] Copyright © 2016 American Chemical Society; (c) Schematic diagram of the ultrahigh frequency (UHF) RFID-based wireless sensor system composed of an RFID sensor tag and RFID-antenna-connected network analyser [80] Copyright © 2015 American Chemical Society.

The detection layer, and especially the type of interaction with the target gas molecules, plays a key role in the detection capabilities of SAW chemical sensors. Therefore, the study of selective coating materials and their properties is of primary interest to many researchers [81–83]. The detection layer of the SAW sensor is the place where the gas adsorbs, which changes the operating frequency, and the higher the frequency, the greater the sensitivity to the target

gas. This change can be up or down. Thus, for example, the pores or grain boundaries of the sensing layer can trap gas molecules, giving a negative frequency shift (-Δf) due to the elastic load. Based on the mass loading effect (proprotional to the amount of absorbed gas), when the gas molecules are adsorbed on the detection layer, a positive frequency shift (+Δf) is obtained [78,81].

Many researchers have designed composites based on organic materials to improve the detection performance of SAW sensors, such as 3D-architecture graphene/ polyvinyl alcohol /SiO_2 (3DAG/PVA/SiO2) to detect moisture [84], MWCNTs to detect ammonia gas [85], PEDOT–CNTs to detect acetone [86], and graphene to detect trinitrotoluene [87], see Table 4. Chen et al [87] studied the effect of IDT electrode materials (graphene and Al) on the sensor response. The results suggest that graphene IDT electrodes have the largest frequency shift and therefore the highest mass sensitivity. This implies that the graphene electrode is a promising candidate for highly sensitive SAW sensor applications.

It is well known that the conductivity of CNTs decreases with exposure to NH_3 and CH_4, which has led to the observation of frequency shifts for a CNT-based resonator when exposed to these gases [85,88]. The change in conductivity (and thus of the imaginary part of the permittivity) affects the amplitude of the resonant frequency, but the frequency shift is related to the change in the real part of the permittivity. One possible explanation is that the interaction of gas molecules with CNTs to create bound charges leads to changes in the real part of the permittivity of CNTs.

The use of TiO_2 and α-Fe_2O_3 nanoparticles in the form of a surface film on a waveguide substrate can improve the sensing detection of NH_3. When these oxides are exposed to NH_3 gas, their permittivity changes, changing the reflection coefficient (S_{11}) and the transmission coefficient (S_{21}). The measurement principle is illustrated in Figure 5.b: a Vector Network Analyser (VNA) was used to send electromagnetic waves to a propagative structure covered

by the sensitive material. The reflection coefficient in detection experiments is equal to the ratio between the amplitude of the reflected wave and that of the incident wave by the sensor at each frequency [79].

Lee et al. [80] introduced a wireless smart sensor system for hydrogen based on Radio Frequency Identification (RFID), consisting of a Pt-decorated reduced graphene oxide (Pt_rGO)-immobilised RFID sensor tag (i.e., signal transfer and signal receiver) and a network analyser connected to an RFID reader antenna to detect hydrogen gas, as shown in Figure 5.c. The loading of noble metals on carbon materials can effectively improve the sensitivity of a sensor. The structure could detect H_2 in the frequency range of 880 to 940 MHz, at concentrations as low as 1 ppm.

Bahoumina et al. [86] used the Inkjet Printing Technology to manufacture a flexible microwave sensor based on PEDOT:PSS-MWCNTs for the detection of ethanol. The structure was printed directly onto a paper substrate using a Dimatix Materials Printer Model DMP-2800. Adsorption of ethanol vapour changes the conductivity of the detection layer. As a result, the resonance frequency and amplitude are shifted. Based on the values extracted at 4 minutes of exposure to ethanol vapours in the range of 0 to 2000 ppm, the sensitivity of the sensor revealed a different resonance frequency estimated at -642.9 Hz/ppm, and the differential amplitude loss was equal to -7 μdB/ppm.

In addition, cellulose nanocrystals have been used as a sensing layer to fabricate an HCl-gas sensor [89], but relative humidity had a significant effect on sensor responses. At 5 ppm, the response frequency was shifted to -32, -96 and -191 kHz at 30, 50 and 85% relative humidity, respectively. The sensor had good sensitivity at low HCl concentrations [89].

Table 4. Summary of SAW gas sensors in terms of materials, targeted gas, propagative structure and response signal at room temperature.

Materials	Gas/Vapour	Propagative structure	frequency range	Response Signal	References

PEDOT–CNTs	Ethanol, C_2H_5OH	Microstrip line	0 to 6 GHz	S parameter (S_{21})	[86]
Cellulose nanocrystals	Hydrogen chloride, HCl	Interdigital transducers	0 to 200 MHz	Resonant frequency	[89]
Beaded activated carbon	Various volatile organic compounds (VOCs) (Formaldehyde, Ethanol , Nitrogen oxides, ...)	Open-ended resonator coupled to input/output microstrip transmission lines	0 to 1550 kHz	Resonant frequency	[90]
Polymethylsiloxane-graftphthalocyanine	Acetone, C_3H_6O	Six-port reflectometer	0 to 10 GHz	S parameter (S_{11}) ΔS_{11}(dB)= 7.32	[91]
Graphene	Nitrogen dioxide, NO_2	Dielectric resonator	-	Central frequency, linewidth (full width at half maximum)	[83]
MWCNTs	Ammonia, NH_3	Coplanar waveguide	0 to 21 GHz	S parameter (S_{21})	[85]
Commercial SAW gas chromatography (GC) analyser	DMMP, $CH_3PO(OCH_3)_2$	Interdigital transducers	0 to 250 kHz	Frequency shifts	[76]
ZnO	DMMP, $CH_3PO(OCH_3)_2$	Dual-delay line configuration	0 to 150 MHz,	S parameter (S_{11})	[78]
ZnO/SiO_2 bi-layer	Ammonia, NH_3	ST-X quartz substrate	0 to200 MHz	Frequency shift	[82]
Metal oxide (ZnO)	Ammonia, NH_3	ST-X quartz substrate	0 to 433 MHz	Frequency shift	[81]
$3DAG/PVA/SiO_2$	Water, H_2O	delay line	0 to 208 MHz	S parameter (S_{21})	[84]
Graphene IDT Aluminium(Al) IDT	Trinitrotoluene, $C_7H_5N_3O_6$	One port SAW resonator	0 to 425 MHz	Frequency shift	[87]

5. Comparison of gas sensors

In this section, we limit ourselves to a comparison of the different types of gas sensor measurements in terms of performance, cost and miniaturisation. The advantages and disadvantages of these different types of gas sensors are listed in Table 5.

Electrochemical and resistive gas sensors offer advantages such as ease of manufacture, simplicity of measurement technology and small size. They are little affected by changes in pressure and temperature. In addition, they measure toxic gases at very low concentrations and have the ability to detect a wide range of gases. Electrochemical sensors have satisfactory sensitivity and selectivity, with short response/recovery times and require very little power to operate. On the other hand, the resistive gas sensor has the common defect of low selectivity and high response/recovery time.

Some of the aforementioned disadvantages can be avoided by using the capacitive measurement technique, which has good selectivity. However, capacitive sensors are limited to PP and IDEs configurations, whereas resistive sensors can be present in various other configurations. In addition, resistive measurements require a DC voltage, whereas capacitive measurements require an AC signal to operate. For portable sensor systems, battery-operated devices (DC input) are preferred. The frequency of the capacitive sensor input signal is used to adjust the sensitivity and selectivity as mentioned above. In addition, the capacitive mode allows the detection of mixed species.

The detection performance of SAW sensors depends on the propagative structure, response signal and detection materials. The SAW sensor generally has good thermal stability, fast response time and good sensitivity. In addition, it can be used for wireless applications with low power consumption. However, it also has limited selectivity, which depends on the availability of detection layers and the higher cost of materials operating at high frequency.

From an efficiency point of view, different measurement techniques are used with different materials and configurations, but no perfect type of sensors has yet been found.

Table 5. Comparison of the main types of gas sensors.

Characteristics	Electrochemical	Capacitive	Resistive	SAW
Cost	Low	High	Low	High
Lifetime	Medium	Long	Long	Good
Selectivity	Medium	Excellent	Poor	Poor
Sensitivity	High	High	High	Good
Response/recovery time	Fast	Fast	Fast	Fast
Size	Medium	Medium	Small	Medium

III. Use of renewable materials in sensors

1. General information

Composites based on organic, and preferably renewable, materials offer excellent advantages in the improvement of electronic devices, such as low cost, low energy consumption and high flexibility. The number of publications and patents related to organic materials in general, and composites based on renewable materials in particular, has increased significantly and continues to grow, as shown in Figure 6.

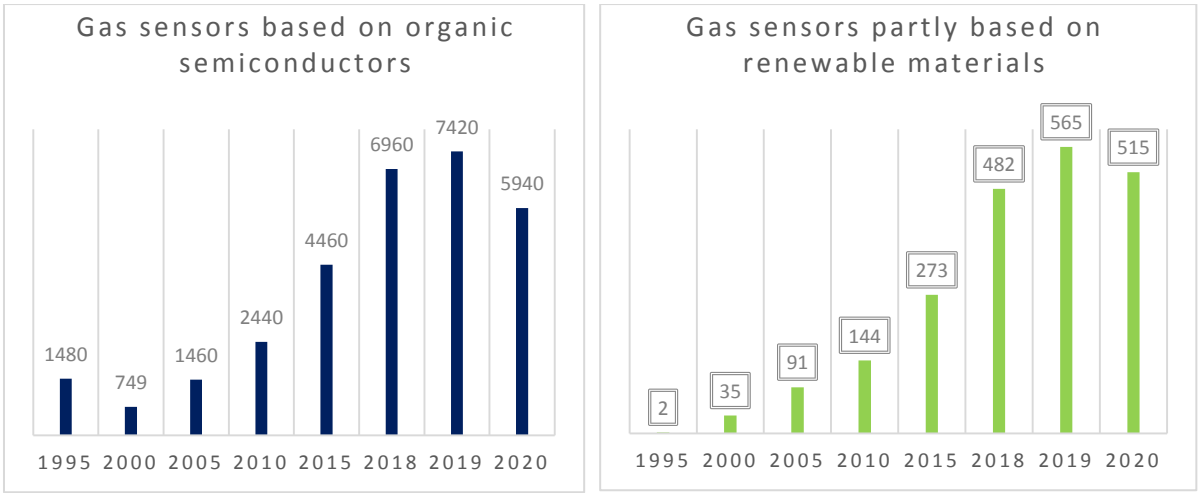

(a) (b)

Figure 6. Evolution of the number of publications on gas sensors: (a) gas sensors based on organic semiconductors, and (b) gas sensors partly based on renewable materials. The decrease in the trend in 2020 is only apparent, as the count was made in the middle of the year.

The combination of basic and technological research has made it possible to produce composite materials partly based on organic materials and biomass derivatives as a solution to minimise environmental, consumption and cost problems. In addition, the characteristics of composite materials can be controlled by varying the combination of constituents of natural origin and/or inorganic/organic nanomaterials. Various studies have been published to provide guidance on their manufacturing process and various applications. Methods for the manufacture of composite materials such as conductive electrode films, cellulose/CNT composite paper, or aerogel, will be discussed in the following paragraphs.

2. Selected examples

Koga et al. [92] proposed a simple process to manufacture a conductive paper based on cellulose nanofibres and conductive nanomaterials such as silver nanowires (AgNWs) and CNTs. In their system, cellulose nanopaper functions both as a filter and as a transparent and flexible substrate. The process of preparing the filtration coating of AgNWs or CNTs on the nanopaper is divided into two steps. The first is to form a wet paper, with the filtration of an aqueous dispersion of cellulose nanofibres using a commercial membrane filter (pore diameter 0.1 mm) for 20 min. The second step is to pour the aqueous dispersion of nanomaterials (either AgNWs or CNTs) onto the wet nanopaper. The wet nanopaper is then filtered by dehydration for 20 min to retain the conductive nanomaterials on the surface. Finally, the nanopaper is dried for 20 min at 110°C using a hot press and then removed from the membrane filter. The filtration coating process gave better results than the spin-coating process. The conductive network was uniformly connected to the vertical drainage through the paper-specific nanopores with strong adhesion to the cellulose substrate.

Han et al. [93] improved the response of the CNT-based humidity sensor by replacing the original glass substrate with a cellulose paper substrate. The sensor based on the cellulose

substrate has indeed shown an excellent response and high robustness to mechanical stresses during bending and folding. Later, the same authors fabricated and compared two ammonia gas sensor structures: (i) the CNT-on-paper made by writing directly on cellulose paper, i.e., a layer-by-layer structure, and (ii) the structure based on the CNT-cellulose composite. These structures can be produced by various methods, including electrospinning, Langmuir–Blodgett deposition, filtration, and spin-coating of dispersed CNT solutions. The CNT-on-paper sensor structure (layer-by-layer structure) has shown shorter response/recovery times than the CNT–cellulose composite structure produced on a glass substrate in a concentration range of 10–100 ppm ammonia [94].

Moreover, the blend of cellulose and CNTs can also be used to make fibres and fibre mats. The manufactured fibres have high mechanical strength and good electrical conductivity to serve various applications. MWCNTs and nano-cellulose can be dissolved in ionic liquids, which can be used as an inspiration for the fibre manufacturing process. Then, subsequent grinding and spinning methods can be used to manufacture fibres with good dispersion and alignment [95,96].

Cho et al. [96] introduced a NO_2 gas sensor based on wearable sensing fibres. To achieve this, nanocellulose extracted from tunicate was homogeneously mixed with SWCNTs to make a Tunicate Cellulose Nanotube Fibres (TCNF) / Carbon Nanotubes (CNT) sensor. The latter exhibited high selectivity and sensitivity, with a detection at the level of the ppb. The (TCNF/CNT) composite fibres were continuously produced in aligned directions by wet spinning, which makes them behave like liquid crystals. The TCNF/CNT-based fibres can be knotted, which gives the possibility to use them in the weaving process and to integrate sensors in smart textiles, as shown in Figure 7.e [96].

Carbonised wood (CW) is also an ideal candidate for creating an electrode material. Teng et al. [97] obtained excellent results with CW as a high-performance product in terms of

cyclability and low cost. CW has good conductivity, open vertical channels and light weight. The transformation of wood into carbon includes various methods such as hydrothermal carbonisation, carbonisation in inert or atmospheric atmosphere, and activation by chemical reagents.

Koga et al. [98] proposed a disposable molecular sensor based on paper substrate, ZnO nanowires, and a graphite electrode created with pencil drawing to detect nitrogen dioxide. The ZnO nanowires implanted on the paper substrate provide highly adhesive lattice structures that allow reliable electrical contact with the electrodes.

In addition, Le et al. [99] presented a new technology for creating a graphene pattern on leaves and wood for green electronics using ultrafast laser pulses. An example of Laser-Induced Graphene (LIG) electronics on a leaf for green electronics is presented in Figure7. a. In turn, Niu et al. [100] used direct laser writing with ultrafast laser pulses to create special conductive graphite arrays or porous patterns from a bio-based material, sodium lignosulfonate (NaLS) as shown in Figure 7.b. Carbon patterns have been successfully applied as piezoresistive and humidity sensors. Laser-induced graphene opens many possibilities for the improvement and development of environmentally friendly devices.

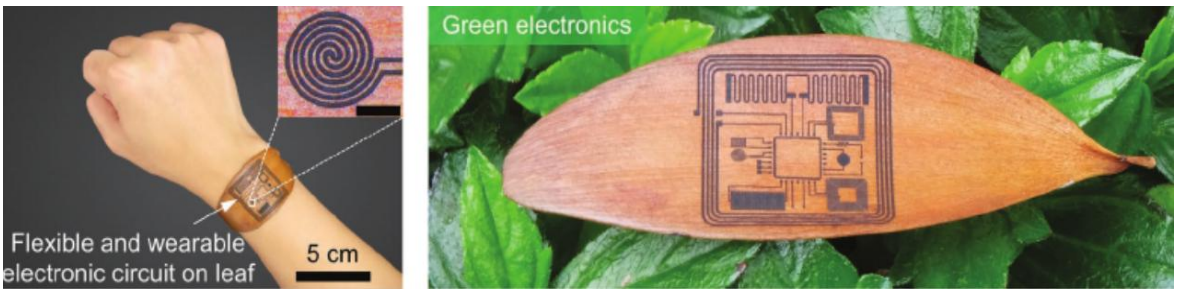

(a)

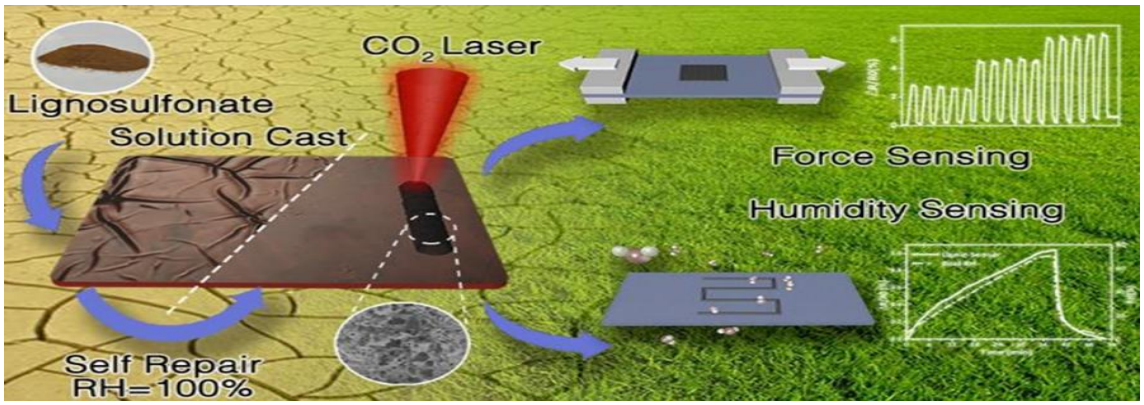

(b)

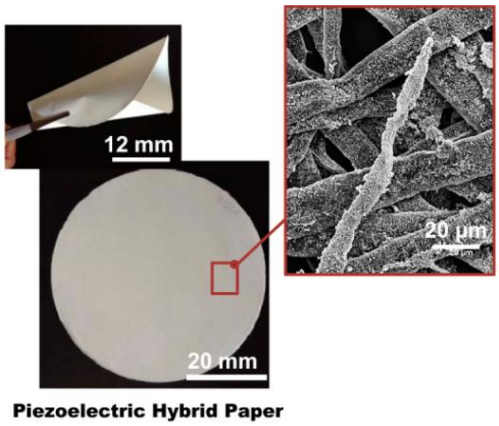

(c)

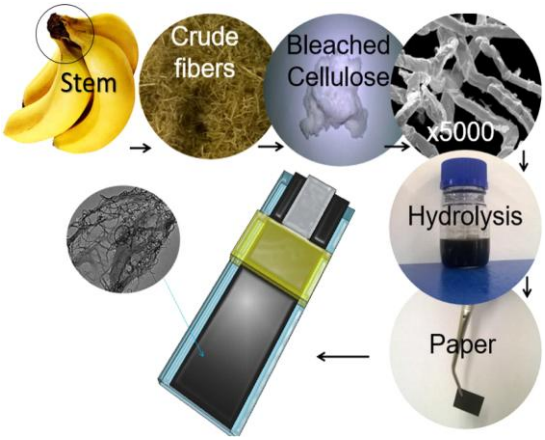

(d)

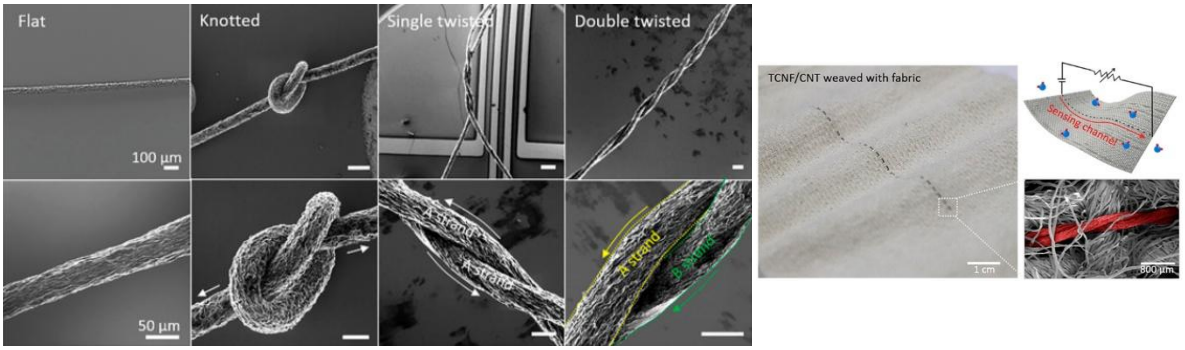

(e)

Figure 7. (a) Photo of laser-induced graphene electronics on a leaf for green electronics [99] copyright Advanced Functional Materials; (b) Green sensor prepared by direct laser writing of modified wood component [100] Copyright © 2019 American Chemical Society; (c) Piezoelectric composite paper based on $BaTiO_3$ on wood cellulose fibres [101] Copyright © 2014 American Chemical Society; (d) Electrode from banana stem [14] with permission from Elsevier; (e) (left) Scanning Electron Microscopy (SEM) images of the flat, knotted, single-twisted and double-twisted TCNF/CNT fibres integrated with sensing devices, and (right) photo, schematic, and SEM image of a TCNF/CNT fibre woven with conventional fabrics [96] Copyright © 2019 American Chemical Society.

Mahadeva et al. [101] have developed a composite piezoelectric paper based on nanostructured $BaTiO_3$ on wood cellulose fibres. The fibre functionalisation process was achieved by a layer-by-layer approach. The surface of the manufactured paper was positively charged, leading to an attractive electrostatic bond with the (negatively charged) $BaTiO_3$, as shown in Figure 7.c. Piezoelectric composite paper has thus shown promising as a low-cost substrate for the realisation of sensing devices [101].

Noremberg et al. [14] used cellulose extracted from a banana stem residue to manufacture a conductive paper containing 5% by weight of oxidised MWCNTs (with –COOH functions). The paper was used for a capacitive methanol gas sensor application, as shown in Figure 7.d. The properties of the paper depend on the size of the cellulose particles and the percentage of MWCNTs [14]. The nature of the cellulose particles, from nanocellulose to microcrystalline cellulose, can be controlled by different methods such as high-energy milling, enzymatic hydrolysis or acid hydrolysis [14,102,103].

On the other hand, In 2020, Sukhavattanakul et al [104] extracted bacterial cellulose nanocrystals from *Gluconacetobacter xylinus* in pellicle using acid hydrolysis. Composite thin films based on nanoparticles of silver (Ag), molybdenumm trioxide (MoO_3) and bacterial cellulose nanocrystals were fabricated for a gas sensor application. When the composite thin film is exposed to H_2S gas, it gives a color change due to redox reactions between gas and MoO_3 nanoparticles. The colour intensity of the suboxide depends on the increase in exposure time and H_2S concentration [104].

Finally, aerogels were also tested for the gas sensor application, which improves the selectivity of resistive gas sensors as they can adsorb specific organic compounds. Qi et al. [105] have thus used cellulose/CNT aerogels for gas sensors. The electrical resistance of NTC/cellulose aerogels changes when exposed to a series of vapours of volatile organic

compounds such as methanol, ethanol, toluene, and others. They exhibit high sensitivity and rapid response [105].

In summary, renewable sources such as wood, plant fibres, bio-based carbon and cellulose, in different forms and from different origins, have largely demonstrated their interest in combination with other materials to make composites. Depending on their combination and manufacturing process, these composite materials can take many forms, such as paper, films, fibres, and aerogels, to serve a variety of applications such as photovoltaic cells, gas sensors, or supercapacitors for example.

IV. Challenges and future directions

1. The challenges

The main challenge of using renewable materials in sensors is to ensure performance in terms of selectivity, sensitivity, response time, stability and operating longevity at low cost. The latter implies improving and increasing sensor operating time, reducing maintenance, lowering installation costs, reducing the costs of analysing system results and managing data, which exceed the cost of developing the sensor itself. For example, to obtain an intelligent sensor with automatic decision making, it is possible to exploit a colour change by using paper-based colorimetric sensor arrays. The colorimetric detection technique measures the colour intensity in relation to the concentration of the analyte. The colour change may be visualised with the naked eye due to enzymatic or chemical reactions [106,107].

As the performance of the sensor system requires an independent assessment of the effects of the environment (e.g. temperature and relative humidity), it is very important to consider these impacts on sensor measurements using, for instance, the following methods: (1) Installation of a dehumidifier prior to the introduction of the target gas into the test chamber

[108,109]; (2) Corrections provided by advanced numerical methods to eliminate the influence of humidity and temperature using a combination of sensor arrays [110,111]; (3) Doping or coating of the sensing layer surface, which are very promising approaches to reduce the dependence of gas sensing characteristics on humidity without sacrificing the gas response. For this purpose, for example, Kim et al. [112] doped hierarchical SnO_2 nanostructures with NiO.

The evolution of technologies such as communication systems and high-frequency microprocessors, IoT, real-time detection and storage capacity, Big Data and wireless communication, can help improving and controlling the quality of our environment, especially in terms of air pollution. The challenge is therefore to successfully integrate and use these technologies in gas detection systems.

In addition, the gas sensor analyser or decision block can be replaced by a simple system such as Arduino® or Raspberry®. The latter are indeed brands of electronic boards on which there is a microcontroller or integrated circuit, a USB port, and input and output connectors that differ according to the models sold on the market, but that can be adapted to be used as a sensor or decision block. Alternatively, a circuit made by Printed Circuit Board (PCB) technology can be used between the smartphone and the sensor's measuring block. A mobile application must then be developed to control and facilitate access and visualisation of the measured data. The data is transferred to the Internet via the mobile application, which can be useful for people suffering from respiratory diseases.

All the economic and technological challenges must convince the scientific communities and decision-makers to support the development of these ideas.

2. The future directions

Different methods and techniques can be used to improve or transform renewable materials into useful low-cost materials with good characteristics such as electrical properties, mechanical strength, high robustness during bending and folding as well as thermal stability and recyclability. These materials can be used in different high value-added applications, such as gas sensors.

Remarkable performance and advances in computer science can also help scientific research on materials by using machine learning algorithms to find optimal parameters, reducing the duration of experiments and the associated costs [113–115]. Similarly, artificial intelligence techniques have been used for a wide variety of research and have allowed machines to mimic imagination. Recently, artificial intelligence has attracted the attention of chemical engineering research. For example, it can help laboratory researchers find the optimal parameters to achieve a useful result and facilitate the process of manufacturing materials [116]. In addition, artificial intelligence can be used in the decision-making part of the detection system to identify the detected gas using non-linear / linear and/or unsupervised / supervised algorithms [117].

In the near future, the microfabrication industry will use 3D-printing technologies that will reduce manufacturing time, facilitate desirable structural design and reduce waste, thereby minimising the cost of the final product [118]. However, the gas sensor detection block is cheaper than the other parts of the detection system. Therefore, the cost of these more expensive parts, such as installation, data analysis, maintenance and sensor integration costs, must be reduced.

Finally, the IoT is widely used as a solution for environmental monitoring and is considered an essential environmental module in the development and sustainability of future smart cities. For example, the GASDUINO system is used to measure the quality of air using the IoT. The GASDUINO is composed of an Arduino® microcontroller board, a gas sensor

(MQ-135®), an Android user interface connected to everything such as IoT, Web server and Wi-Fi, Bluetooth, and Google Cloud Platform via the remote Arduino XY cloud [119]. Reducing system overload and the size of data collected by the sensors requires the use of cryptographic processing algorithms to transmit only the necessary information to the database via wireless communication [120].

V. Conclusion

In this review, different types of gas sensors such as electrochemical, resistive, capacitive and acoustic were discussed and compared. Several works have been presented to show the influence of the nature of materials and structures on sensor performance. It was noted that there is no type of sensors that can be considered perfect. In addition, various research efforts on the development of renewable materials were presented, which have many advantages in terms of ecology, biocompatibility, biodegradability, versatile modification behaviour and natural abundance to preserve our planet. The different development possibilities to obtain an intelligent and inexpensive detection system partly based on renewable materials were presented. Gas sensors based on renewable materials have a satisfactory detection performance. Further progress in this area, and thus broad implementation, will require, in addition to the development of the gas sensor itself, the development of the detection system as a whole (thus including e.g. in addition to the sensor, the acquisition card and the software) and environmental monitoring by combining different research fields such as chemistry, physics, electronics, computer science and embedded system engineering.

Data availability

Not applicable to a review article.

References

[1] M. Donarelli, L. Ottaviano, 2D Materials for Gas Sensing Applications: A Review on Graphene Oxide, MoS2, WS2 and Phosphorene, Sensors. 18 (2018) 3638. https://doi.org/10.3390/s18113638.

[2] M. Karakawa, K. Suzuki, T. Kuwabara, T. Taima, K. Nagai, M. Nakano, T. Yamaguchi, K. Takahashi, Factors contributing to degradation of organic photovoltaic cells, Org. Electron. 76 (2020) 105448. https://doi.org/10.1016/j.orgel.2019.105448.

[3] Z. Yang, J. Tian, Z. Yin, C. Cui, W. Qian, F. Wei, Carbon nanotube- and graphene-based nanomaterials and applications in high-voltage supercapacitor: A review, Carbon N. Y. 141 (2019) 467–480. https://doi.org/10.1016/j.carbon.2018.10.010.

[4] H. Chen, W. Zhang, M. Li, G. He, X. Guo, Interface Engineering in Organic Field-Effect Transistors: Principles, Applications, and Perspectives, Chem. Rev. 120 (2020) 2879–2949. https://doi.org/10.1021/acs.chemrev.9b00532.

[5] S.Z.N. Demon, A.I. Kamisan, N. Abdullah, S.A.M. Noor, O.K. Khim, N.A.M. Kasim, M.Z.A. Yahya, N.A.A. Manaf, A.F.M. Azmi, N.A. Halim, Graphene-based Materials in Gas Sensor Applications: A Review, Sensors Mater. 32 (2020) 759. https://doi.org/10.18494/SAM.2020.2492.

[6] H.S. Hong, N.H. Phuong, N.T. Huong, N.H. Nam, N.T. Hue, Highly sensitive and low detection limit of resistive NO2 gas sensor based on a MoS2/graphene two-dimensional heterostructures, Appl. Surf. Sci. 492 (2019) 449–454. https://doi.org/10.1016/j.apsusc.2019.06.230.

[7] J.H. Choi, J. Lee, M. Byeon, T.E. Hong, H. Park, C.Y. Lee, Graphene-Based Gas Sensors with High Sensitivity and Minimal Sensor-to-Sensor Variation, ACS Appl.

Nano Mater. (2020). https://doi.org/10.1021/acsanm.9b02378.

[8] A. Nasri, A. Boubaker, B. Hafsi, W. Khaldi, A. Kalboussi, High-Sensitivity Sensor Using C 60 -Single Molecule Transistor, IEEE Sens. J. 18 (2018) 248–254. https://doi.org/10.1109/JSEN.2017.2769803.

[9] M.I. Mead, O.A.M. Popoola, G.B. Stewart, P. Landshoff, M. Calleja, M. Hayes, J.J. Baldovi, M.W. McLeod, T.F. Hodgson, J. Dicks, A. Lewis, J. Cohen, R. Baron, J.R. Saffell, R.L. Jones, The use of electrochemical sensors for monitoring urban air quality in low-cost, high-density networks, Atmos. Environ. 70 (2013) 186–203. https://doi.org/10.1016/j.atmosenv.2012.11.060.

[10] G. Gregis, J.-B. Sanchez, I. Bezverkhyy, W. Guy, F. Berger, V. Fierro, J.-P. Bellat, A. Celzard, Detection and quantification of lung cancer biomarkers by a micro-analytical device using a single metal oxide-based gas sensor, Sensors Actuators B Chem. 255 (2018) 391–400. https://doi.org/10.1016/j.snb.2017.08.056.

[11] G. Barandun, M. Soprani, S. Naficy, M. Grell, M. Kasimatis, K.L. Chiu, A. Ponzoni, F. Güder, Cellulose Fibers Enable Near-Zero-Cost Electrical Sensing of Water-Soluble Gases, ACS Sensors. 4 (2019) 1662–1669. https://doi.org/10.1021/acssensors.9b00555.

[12] Z. Yuan, J. Zhao, F. Meng, W. Qin, Y. Chen, M. Yang, M. Ibrahim, Y. Zhao, Sandwich-like composites of double-layer Co3O4 and reduced graphene oxide and their sensing properties to volatile organic compounds, J. Alloys Compd. 793 (2019) 24–30. https://doi.org/10.1016/j.jallcom.2019.03.386.

[13] Z. Yuan, E. Han, F. Meng, K. Zuo, Detection and Identification of Volatile Organic Compounds Based on Temperature-Modulated ZnO Sensors, IEEE Trans. Instrum. Meas. 69 (2020) 4533–4544. https://doi.org/10.1109/TIM.2019.2948413.

[14] B.S. Noremberg, R.M. Silva, O.G. Paniz, J.H. Alano, M.R.F. Gonçalves, S.I. Wolke, J.

Labidi, A. Valentini, N.L.V. Carreño, From banana stem to conductive paper: A capacitive electrode and gas sensor, Sensors Actuators, B Chem. 240 (2017) 459–467. https://doi.org/10.1016/j.snb.2016.09.014.

[15] Y. Deng, Y. Deng, Sensing Mechanism and Evaluation Criteria of Semiconducting Metal Oxides Gas Sensors, in: Semicond. Met. Oxides Gas Sens., Springer Singapore, 2019: pp. 23–51. https://doi.org/10.1007/978-981-13-5853-1_2.

[16] G.W. Hunter, S. Akbar, S. Bhansali, M. Daniele, P.D. Erb, K. Johnson, C.-C. Liu, D. Miller, O. Oralkan, P.J. Hesketh, P. Manickam, R.L. Vander Wal, Editors' Choice—Critical Review—A Critical Review of Solid State Gas Sensors, J. Electrochem. Soc. 167 (2020) 037570. https://doi.org/10.1149/1945-7111/ab729c.

[17] M.A. Najeeb, Z. Ahmad, R.A. Shakoor, Organic Thin-Film Capacitive and Resistive Humidity Sensors: A Focus Review, Adv. Mater. Interfaces. 5 (2018) 1800969. https://doi.org/10.1002/admi.201800969.

[18] W.R. HEINEMAN, Electrochemical Sensors, Electrochemistry. 74 (2006) 105. https://doi.org/10.5796/electrochemistry.74.105.

[19] A.M. VinuMohan, Screen-Printed Electrochemical Sensors for Environmental Contaminants, in: 2020: pp. 85–108. https://doi.org/10.1007/978-3-030-45116-5_5.

[20] D. Tyagi, H. Wang, W. Huang, L. Hu, Y. Tang, Z. Guo, Z. Ouyang, H. Zhang, Recent advances in two-dimensional-material-based sensing technology toward health and environmental monitoring applications, Nanoscale. 12 (2020) 3535–3559. https://doi.org/10.1039/C9NR10178K.

[21] M.A. Rahman, P. Kumar, D.S. Park, Y.B. Shim, Electrochemical sensors based on organic conjugated polymers, Sensors. 8 (2008) 118–141. https://doi.org/10.3390/s8010118.

[22] P. Wei, Z. Ning, S. Ye, L. Sun, F. Yang, K.C. Wong, D. Westerdahl, P.K.K. Louie, Impact analysis of temperature and humidity conditions on electrochemical sensor response in ambient air quality monitoring, Sensors (Switzerland). 18 (2018). https://doi.org/10.3390/s18020059.

[23] Z. Yuan, R. Li, F. Meng, J. Zhang, K. Zuo, E. Han, Approaches to enhancing gas sensing properties: A review, Sensors (Switzerland). 19 (2019). https://doi.org/10.3390/s19071495.

[24] H. Chu, Y. Shen, L. Lin, X. Qin, G. Feng, Z. Lin, J. Wang, H. Liu, Y. Li, Ionic-liquid-assisted preparation of carbon nanotube-supported uniform noble metal nanoparticles and their enhanced catalytic performance, in: Adv. Funct. Mater., 2010: pp. 3747–3752. https://doi.org/10.1002/adfm.201001240.

[25] T. Hyodo, M. Takamori, T. Goto, T. Ueda, Y. Shimizu, Potentiometric CO sensors using anion-conducting polymer electrolyte: Effects of the kinds of noble metal-loaded metal oxides as sensing-electrode materials on CO-sensing properties, Sensors Actuators, B Chem. 287 (2019) 42–52. https://doi.org/10.1016/j.snb.2019.02.036.

[26] C. Flores-Rodriguez, C. Nagendranatha Reddy, B. Min, Enhanced methane production from acetate intermediate by bioelectrochemical anaerobic digestion at optimal applied voltages, Biomass and Bioenergy. 127 (2019). https://doi.org/10.1016/j.biombioe.2019.105261.

[27] L. Yang, C. Xu, W. Ye, W. Liu, An electrochemical sensor for H2O2 based on a new Co-metal-organic framework modified electrode, Sensors Actuators, B Chem. 215 (2015) 489–496. https://doi.org/10.1016/j.snb.2015.03.104.

[28] P. Kuberský, T. Syrový, A. Hamacek, S. Nešpůrek, J. Stejskal, Printed flexible gas sensors based on organic materials, in: Procedia Eng., Elsevier Ltd, 2015: pp. 614–617.

https://doi.org/10.1016/j.proeng.2015.08.746.

[29] Y. Dan, Y. Lu, N.J. Kybert, Z. Luo, A.T.C. Johnson, Intrinsic response of graphene vapor sensors, Nano Lett. 9 (2009) 1472–1475. https://doi.org/10.1021/nl8033637.

[30] E. Song, R.P. Tortorich, T.H. da Costa, J.-W. Choi, Inkjet printing of conductive polymer nanowire network on flexible substrates and its application in chemical sensing, Microelectron. Eng. 145 (2015) 143–148. https://doi.org/10.1016/j.mee.2015.04.004.

[31] D.K. Bandgar, S.T. Navale, A.T. Mane, S.K. Gupta, D.K. Aswal, V.B. Patil, Ammonia sensing properties of polyaniline/α-Fe2O3 hybrid nanocomposites, Synth. Met. 204 (2015) 1–9. https://doi.org/10.1016/j.synthmet.2015.02.032.

[32] G.D. Khuspe, S.T. Navale, M.A. Chougule, V.B. Patil, Ammonia gas sensing properties of CSA doped PANi-SnO2 nanohybrid thin films, Synth. Met. 185–186 (2013) 1–8. https://doi.org/10.1016/j.synthmet.2013.09.032.

[33] Z. Wu, X. Chen, S. Zhu, Z. Zhou, Y. Yao, W. Quan, B. Liu, Enhanced sensitivity of ammonia sensor using graphene/polyaniline nanocomposite, Sensors Actuators B Chem. 178 (2013) 485–493. https://doi.org/10.1016/j.snb.2013.01.014.

[34] SGX Sensortech, Gas Sensor & Detector Technology Leaders | SGX Sensortech, (n.d.). https://www.sgxsensortech.com/ (accessed June 18, 2020).

[35] Figaro Engineering Inc, Operating principle - Electrochemical-type gas sensor, (n.d.). https://www.figaro.co.jp/en/technicalinfo/principle/electrochemical-type.html (accessed June 18, 2020).

[36] T. Syrový, P. Kuberský, I. Sapurina, S. Pretl, P. Bober, L. Syrová, A. Hamáček, J. Stejskal, Gravure-printed ammonia sensor based on organic polyaniline colloids, Sensors Actuators, B Chem. 225 (2016) 510–516.

https://doi.org/10.1016/j.snb.2015.11.062.

[37] H. Wan, Y. Gan, J. Sun, T. Liang, S. Zhou, P. Wang, High sensitive reduced graphene oxide-based room temperature ionic liquid electrochemical gas sensor with carbon-gold nanocomposites amplification, Sensors Actuators B Chem. 299 (2019) 126952. https://doi.org/10.1016/j.snb.2019.126952.

[38] J. Liao, H. Si, X. Zhang, S. Lin, Functional Sensing Interfaces of PEDOT:PSS Organic Electrochemical Transistors for Chemical and Biological Sensors: A Mini Review, Sensors. 19 (2019) 218. https://doi.org/10.3390/s19020218.

[39] A. Kumar, P. Jha, A. Singh, A.K. Chauhan, S.K. Gupta, D.K. Aswal, K.P. Muthe, S.C. Gadkari, Modeling of gate bias controlled NO2 response of the PCDTBT based organic field effect transistor, Chem. Phys. Lett. 698 (2018) 7–10. https://doi.org/10.1016/j.cplett.2018.02.043.

[40] W. Hai, T. Goda, H. Takeuchi, S. Yamaoka, Y. Horiguchi, A. Matsumoto, Y. Miyahara, Human influenza virus detection using sialyllactose-functionalized organic electrochemical transistors, Sensors Actuators B Chem. 260 (2018) 635–641. https://doi.org/10.1016/j.snb.2018.01.081.

[41] R.-X. He, M. Zhang, F. Tan, P.H.M. Leung, X.-Z. Zhao, H.L.W. Chan, M. Yang, F. Yan, Detection of bacteria with organic electrochemical transistors, J. Mater. Chem. 22 (2012) 22072. https://doi.org/10.1039/c2jm33667g.

[42] J. Liu, M. Agarwal, K. Varahramyan, Glucose sensor based on organic thin film transistor using glucose oxidase and conducting polymer, Sensors Actuators B Chem. 135 (2008) 195–199. https://doi.org/10.1016/j.snb.2008.08.009.

[43] D. Acharyya, P. Bhattacharyya, Alcohol sensing performance of ZnO hexagonal nanotubes at low temperatures: A qualitative understanding, Sensors Actuators, B

Chem. 228 (2016) 373–386. https://doi.org/10.1016/j.snb.2016.01.035.

[44] A. Hazra, K. Dutta, B. Bhowmik, P.P. Chattopadhyay, P. Bhattacharyya, Room temperature alcohol sensing by oxygen vacancy controlled TiO 2 nanotube array, Appl. Phys. Lett. 105 (2014). https://doi.org/10.1063/1.4894008.

[45] J. Yu, X. Yu, L. Zhang, H. Zeng, Ammonia gas sensor based on pentacene organic field-effect transistor, Sensors Actuators, B Chem. 173 (2012) 133–138. https://doi.org/10.1016/j.snb.2012.06.060.

[46] C. Wang, L. Zhang, H. Huang, R. Xi, D.-P. Jiang, S.-H. Zhang, L.-J. Wang, Z.-Y. Chen, G.-B. Pan, A nanocomposite consisting of ZnO decorated graphene oxide nanoribbons for resistive sensing of NO2 gas at room temperature, Microchim. Acta. 186 (2019). https://doi.org/10.1007/s00604-019-3628-x.

[47] Y. Seekaew, A. Wisitsoraat, D. Phokharatkul, C. Wongchoosuk, Room temperature toluene gas sensor based on TiO2 nanoparticles decorated 3D graphene-carbon nanotube nanostructures, Sensors Actuators B Chem. 279 (2019) 69–78. https://doi.org/10.1016/j.snb.2018.09.095.

[48] Z. Gao, Z. Lou, S. Chen, L. Li, K. Jiang, Z. Fu, W. Han, G. Shen, Fiber gas sensor-integrated smart face mask for room-temperature distinguishing of target gases, Nano Res. 11 (2018) 511–519. https://doi.org/10.1007/s12274-017-1661-9.

[49] B. Liu, X. Liu, Z. Yuan, Y. Jiang, Y. Su, J. Ma, H. Tai, A flexible NO2 gas sensor based on polypyrrole/nitrogen-doped multiwall carbon nanotube operating at room temperature, Sensors Actuators B Chem. 295 (2019) 86–92. https://doi.org/10.1016/j.snb.2019.05.065.

[50] T. Wang, D. Huang, Z. Yang, S. Xu, G. He, X. Li, N. Hu, G. Yin, D. He, L. Zhang, A Review on Graphene-Based Gas/Vapor Sensors with Unique Properties and Potential

Applications, Nano-Micro Lett. 8 (2016) 95–119. https://doi.org/10.1007/s40820-015-0073-1.

[51] G. Lu, L.E. Ocola, J. Chen, Room-Temperature Gas Sensing Based on Electron Transfer between Discrete Tin Oxide Nanocrystals and Multiwalled Carbon Nanotubes, Adv. Mater. 21 (2009) 2487–2491. https://doi.org/10.1002/adma.200803536.

[52] H. Long, A. Harley-Trochimczyk, T. Pham, Z. Tang, T. Shi, A. Zettl, C. Carraro, M.A. Worsley, R. Maboudian, High Surface Area MoS 2 /Graphene Hybrid Aerogel for Ultrasensitive NO 2 Detection, Adv. Funct. Mater. 26 (2016) 5158–5165. https://doi.org/10.1002/adfm.201601562.

[53] K.H. An, S.Y. Jeong, H.R. Hwang, Y.H. Lee, Enhanced sensitivity of a gas sensor incorporating single-walled carbon nanotube-polypyrrole nanocomposites, Adv. Mater. 16 (2004) 1005–1009. https://doi.org/10.1002/adma.200306176.

[54] W. Kim, S. Cho, J.S. Lee, Comparative Study on the Effect of Protonation Control for Resistive Gas Sensor Based on Close-Packed Polypyrrole Nanoparticles, Appl. Sci. 10 (2020) 1850. https://doi.org/10.3390/app10051850.

[55] H.-L. Wei, P. Kumar, D.-J. Yao, Printed Resistive Sensor Array Combined with a Flexible Substrate for Ethanol and Methane Detection, ECS J. Solid State Sci. Technol. 9 (2020) 115008. https://doi.org/10.1149/2162-8777/ab9fe6.

[56] K. Kaviyarasu, G.T. Mola, S.O. Oseni, K. Kanimozhi, C.M. Magdalane, J. Kennedy, M. Maaza, ZnO doped single wall carbon nanotube as an active medium for gas sensor and solar absorber, J. Mater. Sci. Mater. Electron. 30 (2019) 147–158. https://doi.org/10.1007/s10854-018-0276-6.

[57] K. Dutta, N. Banerjee, H. Mishra, P. Bhattacharyya, Performance Improvement of

Pd/ZnO-NR/Si MIS Gas Sensor Device in Capacitive Mode: Correlation with Equivalent-Circuit Elements, IEEE Trans. Electron Devices. 63 (2016) 1266–1273. https://doi.org/10.1109/TED.2016.2520020.

[58] K. Dutta, B. Bhowmik, P. Bhattacharyya, Resonant Frequency Tuning Technique for Selective Detection of Alcohols by TiO2 Nanorod-Based Capacitive Device, IEEE Trans. Nanotechnol. 16 (2017) 820–825. https://doi.org/10.1109/TNANO.2017.2670661.

[59] Y. Chen, F. Meng, M. Li, J. Liu, Novel capacitive sensor: Fabrication from carbon nanotube arrays and sensing property characterization, Sensors Actuators, B Chem. 140 (2009) 396–401. https://doi.org/10.1016/j.snb.2009.04.012.

[60] V. Vizcaino, M. Jelisavcic, J.P. Sullivan, S.J. Buckman, Elastic electron scattering from formic acid (HCOOH): Absolute differential cross-sections, New J. Phys. 8 (2006). https://doi.org/10.1088/1367-2630/8/6/085.

[61] M.K. Filippidou, M. Chatzichristidi, S. Chatzandroulis, Filippidou et al, M.K. Filippidou, M. Chatzichristidi, S. Chatzandroulis, Filippidou et al, A fabrication process of flexible IDE capacitive chemical sensors using a two step lift-off method based on PVA patterning, Sensors Actuators, B Chem. 284 (2019) 7–12. https://doi.org/10.1016/j.snb.2018.12.095.

[62] M.A. Andrés, M.T. Vijjapu, S.G. Surya, O. Shekhah, K.N. Salama, C. Serre, M. Eddaoudi, O. Roubeau, I. Gascón, Methanol and Humidity Capacitive Sensors Based on Thin Films of MOF Nanoparticles, ACS Appl. Mater. Interfaces. 12 (2020) 4155–4162. https://doi.org/10.1021/acsami.9b20763.

[63] J. Paul, J. Philip, Inter-digital capacitive ethanol sensor coated with cobalt ferrite nano composite as gas sensing material, Mater. Today Proc. 25 (2020) 148–150.

https://doi.org/10.1016/j.matpr.2019.12.247.

[64] S. Pourteimoor, H. Haratizadeh, Performance of a fabricated nanocomposite-based capacitive gas sensor at room temperature, J. Mater. Sci. Mater. Electron. 28 (2017) 18529–18534. https://doi.org/10.1007/s10854-017-7800-y.

[65] F.L. Meng, L. Zhang, Y. Jia, J.Y. Liu, Y.F. Sun, T. Luo, M.Q. Li, J.H. Liu, X.J. Huang, Electronic chip based on self-oriented carbon nanotube microelectrode array to enhance the sensitivity of indoor air pollutants capacitive detection, Sensors Actuators, B Chem. 153 (2011) 103–109. https://doi.org/10.1016/j.snb.2010.10.011.

[66] H. Bi, K. Yin, X. Xie, J. Ji, S. Wan, L. Sun, M. Terrones, M.S. Dresselhaus, Ultrahigh humidity sensitivity of graphene oxide, Sci. Rep. 3 (2013) 2714. https://doi.org/10.1038/srep02714.

[67] N.A. Roslan, A. Abu Bakar, T.M. Bawazeer, M.S. Alsoufi, N. Alsenany, W.H. Abdul Majid, A. Supangat, Enhancing the performance of vanadyl phthalocyanine-based humidity sensor by varying the thickness, Sensors Actuators, B Chem. 279 (2019) 148–156. https://doi.org/10.1016/j.snb.2018.09.109.

[68] S. Zeinali, S. Homayoonnia, G. Homayoonnia, Comparative investigation of interdigitated and parallel-plate capacitive gas sensors based on Cu-BTC nanoparticles for selective detection of polar and apolar VOCs indoors, Sensors Actuators, B Chem. 278 (2019) 153–164. https://doi.org/10.1016/j.snb.2018.07.006.

[69] Lord Rayleigh, On Waves Propagated along the Plane Surface of an Elastic Solid, Proc. London Math. Soc. s1-17 (1885) 4–11. https://doi.org/10.1112/plms/s1-17.1.4.

[70] S. El Bouazzaoui, M.E. Achour, C. Brosseau, Microwave effective permittivity of carbon black filled polymers: Comparison of mixing law and effective medium equation predictions, J. Appl. Phys. 110 (2011). https://doi.org/10.1063/1.3644947.

[71] X. Huang, T. Leng, T. Georgiou, J. Abraham, R. Raveendran Nair, K.S. Novoselov, Z. Hu, Graphene Oxide Dielectric Permittivity at GHz and Its Applications for Wireless Humidity Sensing, Sci. Rep. 8 (2018) 43. https://doi.org/10.1038/s41598-017-16886-1.

[72] J. George, A. Abdelghani, P. Bahoumina, O. Tantot, D. Baillargeat, K. Frigui, S. Bila, H. Hallil, C. Dejous, CNT-Based Inkjet-Printed RF Gas Sensor: Modification of Substrate Properties during the Fabrication Process, Sensors. 19 (2019) 1768. https://doi.org/10.3390/s19081768.

[73] C. Xie, A.R. Oganov, D. Dong, N. Liu, D. Li, T.T. Debela, Rational design of inorganic dielectric materials with expected permittivity, Sci. Rep. 5 (2015). https://doi.org/10.1038/srep16769.

[74] S.M. Auerbach, K.A. Carrado, P.K. Dutta, Handbook of Zeolite Science and Technology, M. Dekker, 2003. https://doi.org/10.1201/9780203911167.

[75] S.L. Hietala, D.M. Smith, V.M. Hietala, G.C. Frye, S.J. Martin, Pore structure characterization of thin films using a surface acoustic wave/volumetric adsorption technique, Langmuir. 9 (1993) 249–251. https://doi.org/10.1021/la00025a047.

[76] J. Liu, Y. Lu, Response Mechanism for Surface Acoustic Wave Gas Sensors Based on Surface-Adsorption, Sensors. 14 (2014) 6844–6853. https://doi.org/10.3390/s140406844.

[77] C.H. Wilcox, Perturbation Theory for Linear Operators, 1970. https://doi.org/10.1137/1012029.

[78] X. Qi, J. Liu, Y. Liang, J. Li, S. He, The response mechanism of surface acoustic wave gas sensors in real time, Jpn. J. Appl. Phys. 58 (2019) 014001. https://doi.org/10.7567/1347-4065/aaf223.

[79] G. Bailly, J. Rossignol, B. de Fonseca, P. Pribetich, D. Stuerga, Microwave Gas

Sensing with Hematite: Shape Effect on Ammonia Detection Using Pseudocubic, Rhombohedral, and Spindlelike Particles, ACS Sensors. 1 (2016) 656–662. https://doi.org/10.1021/acssensors.6b00297.

[80] J.S. Lee, J. Oh, J. Jun, J. Jang, Wireless Hydrogen Smart Sensor Based on Pt/Graphene-Immobilized Radio-Frequency Identification Tag, ACS Nano. 9 (2015) 7783–7790. https://doi.org/10.1021/acsnano.5b02024.

[81] V.B. Raj, H. Singh, A.T.T. Nimal, M.U.U. Sharma, M. Tomar, V. Gupta, Distinct detection of liquor ammonia by ZnO/SAW sensor: Study of complete sensing mechanism, Sensors Actuators B Chem. 238 (2017) 83–90. https://doi.org/10.1016/j.snb.2016.07.040.

[82] Y.-L.L. Tang, Z.-J.J. Li, J.-Y.Y. Ma, Y.-J.J. Guo, Y.-Q.Q. Fu, X.-T.T. Zu, Ammonia gas sensors based on ZnO/SiO2 bi-layer nanofilms on ST-cut quartz surface acoustic wave devices, Sensors Actuators B Chem. 201 (2014) 114–121. https://doi.org/10.1016/j.snb.2014.04.046.

[83] N.C.G. Black, I. Rungger, B. Li, S.A. Maier, L.F. Cohen, J.C. Gallop, L. Hao, Adsorption dynamics of CVD graphene investigated by a contactless microwave method, 2D Mater. 5 (2018) 035024. https://doi.org/10.1088/2053-1583/aac231.

[84] Y. Su, C. Li, M. Li, H. Li, S. Xu, L. Qian, B. Yang, Surface acoustic wave humidity sensor based on three-dimensional architecture graphene/PVA/SiO2 and its application for respiration monitoring, Sensors Actuators B Chem. 308 (2020) 127693. https://doi.org/10.1016/j.snb.2020.127693.

[85] A. Cismaru, M. Aldrigo, A. Radoi, M. Dragoman, Carbon nanotube-based electromagnetic band gap resonator for CH 4 gas detection, J. Appl. Phys. 119 (2016) 124504. https://doi.org/10.1063/1.4944708.

[86] P. Bahoumina, H. Hallil, J.L.L. Lachaud, A. Abdelghani, K. Frigui, S. Bila, D. Baillargeat, A. Ravichandran, P. Coquet, C. Paragua, E. Pichonat, H. Happy, D. Rebière, C. Dejous, Microwave flexible gas sensor based on polymer multi wall carbon nanotubes sensitive layer, Sensors Actuators B Chem. 249 (2017) 708–714. https://doi.org/10.1016/j.snb.2017.04.127.

[87] C. Chen, J. Jin, Surface Acoustic Wave Vapor Sensor with Graphene Interdigital Transducer for TNT Detection, Sens. Imaging. 21 (2020) 24. https://doi.org/10.1007/s11220-020-00287-2.

[88] C. Occhiuzzi, A. Rida, G. Marrocco, M. Tentzeris, RFID Passive Gas Sensor Integrating Carbon Nanotubes, IEEE Trans. Microw. Theory Tech. 59 (2011) 2674–2684. https://doi.org/10.1109/TMTT.2011.2163416.

[89] Y. Tang, X. Xu, H. Du, H. Zhu, D. Li, D. Ao, Y. Guo, Y.Q. Fu, X. Zu, Cellulose nano-crystals as a sensitive and selective layer for high performance surface acoustic wave HCl gas sensors, Sensors Actuators, A Phys. 301 (2020) 111792. https://doi.org/10.1016/j.sna.2019.111792.

[90] M. Fayaz, M. Jahandar Lashaki, M. Abdolrazzaghi, M.H. Zarifi, Z. Hashisho, M. Daneshmand, J.E. Anderson, M. Nichols, Monitoring the residual capacity of activated carbon in an emission abatement system using a non-contact, high resolution microwave resonator sensor, Sensors Actuators, B Chem. 282 (2019) 218–224. https://doi.org/10.1016/j.snb.2018.11.038.

[91] K. Staszek, A. Rydosz, E. Maciak, K. Wincza, S. Gruszczynski, Six-port microwave system for volatile organic compounds detection, Sensors Actuators, B Chem. 245 (2017) 882–894. https://doi.org/10.1016/j.snb.2017.01.194.

[92] H. Koga, M. Nogi, N. Komoda, T.T. Nge, T. Sugahara, K. Suganuma, Uniformly

connected conductive networks on cellulose nanofiber paper for transparent paper electronics, NPG Asia Mater. 6 (2014) 1–8. https://doi.org/10.1038/am.2014.9.

[93] J.W. Han, B. Kim, J. Li, M. Meyyappan, Carbon nanotube based humidity sensor on cellulose paper, J. Phys. Chem. C. 116 (2012) 22094–22097. https://doi.org/10.1021/jp3080223.

[94] J.-W. Han, B. Kim, J. Li, M. Meyyappan, A carbon nanotube based ammonia sensor on cellulose paper, RSC Adv. 4 (2014) 549–553. https://doi.org/10.1039/C3RA46347H.

[95] R.K. Mishra, P. Mishra, K. Verma, A. Mondal, R.G. Chaudhary, M.M. Abolhasani, S. Loganathan, Electrospinning production of nanofibrous membranes, Springer International Publishing, 2019. https://doi.org/10.1007/s10311-018-00838-w.

[96] S.Y. Cho, H. Yu, J. Choi, H. Kang, S. Park, J.S. Jang, H.J. Hong, I.D. Kim, S.K. Lee, H.S. Jeong, H.T. Jung, Continuous Meter-Scale Synthesis of Weavable Tunicate Cellulose/Carbon Nanotube Fibers for High-Performance Wearable Sensors, ACS Nano. 13 (2019) 9332–9341. https://doi.org/10.1021/acsnano.9b03971.

[97] S. Teng, G. Siegel, W. Wang, A. Tiwari, Carbonized wood for supercapacitor electrodes, ECS Solid State Lett. 3 (2014) M25–M28. https://doi.org/10.1149/2.005405ssl.

[98] H. Koga, K. Nagashima, Y. Huang, G. Zhang, C. Wang, T. Takahashi, A. Inoue, H. Yan, M. Kanai, Y. He, K. Uetani, M. Nogi, T. Yanagida, Paper-Based Disposable Molecular Sensor Constructed from Oxide Nanowires, Cellulose Nanofibers, and Pencil-Drawn Electrodes, ACS Appl. Mater. Interfaces. 11 (2019) 15044–15050. https://doi.org/10.1021/acsami.9b01287.

[99] T.S.D. Le, S. Park, J. An, P.S. Lee, Y.J. Kim, Ultrafast Laser Pulses Enable One-Step Graphene Patterning on Woods and Leaves for Green Electronics, Adv. Funct. Mater.

29 (2019) 1–10. https://doi.org/10.1002/adfm.201902771.

[100] M. Niu, Y. Yao, Y. Shi, J. Luo, X. Duan, T. Liu, X. Guo, Multifunctional Green Sensor Prepared by Direct Laser Writing of Modified Wood Component, Ind. Eng. Chem. Res. 58 (2019) 10364–10372. https://doi.org/10.1021/acs.iecr.9b00850.

[101] S.K. Mahadeva, K. Walus, B. Stoeber, Piezoelectric paper fabricated via nanostructured barium titanate functionalization of wood cellulose fibers, ACS Appl. Mater. Interfaces. 6 (2014) 7547–7553. https://doi.org/10.1021/am5008968.

[102] E.H. Qua, P.R. Hornsby, H.S.S. Sharma, G. Lyons, Preparation and characterisation of cellulose nanofibres, J. Mater. Sci. 46 (2011) 6029–6045. https://doi.org/10.1007/s10853-011-5565-x.

[103] M. Jorfi, E.J. Foster, Recent advances in nanocellulose for biomedical applications, J. Appl. Polym. Sci. 132 (2015) n/a-n/a. https://doi.org/10.1002/app.41719.

[104] P. Sukhavattanakul, H. Manuspiya, Fabrication of hybrid thin film based on bacterial cellulose nanocrystals and metal nanoparticles with hydrogen sulfide gas sensor ability, Carbohydr. Polym. 230 (2020) 115566. https://doi.org/10.1016/j.carbpol.2019.115566.

[105] H. Qi, J. Liu, J. Pionteck, P. Pötschke, E. Mäder, Carbon nanotube–cellulose composite aerogels for vapour sensing, Sensors Actuators B Chem. 213 (2015) 20–26. https://doi.org/10.1016/j.snb.2015.02.067.

[106] D.D. Liana, B. Raguse, J.J. Gooding, E. Chow, Recent Advances in Paper-Based Sensors, Sensors. 12 (2012) 11505–11526. https://doi.org/10.3390/s120911505.

[107] Y. Chen, G. Fu, Y. Zilberman, W. Ruan, S.K. Ameri, Y.S. Zhang, E. Miller, S.R. Sonkusale, Low cost smart phone diagnostics for food using paper-based colorimetric sensor arrays, Food Control. 82 (2017) 227–232. https://doi.org/10.1016/j.foodcont.2017.07.003.

[108] R. Xing, Q. Li, L. Xia, J. Song, L. Xu, J. Zhang, Y. Xie, H. Song, Au-modified three-dimensional In2O3 inverse opals: synthesis and improved performance for acetone sensing toward diagnosis of diabetes, Nanoscale. 7 (2015) 13051–13060. https://doi.org/10.1039/c5nr02709h.

[109] K. Kawamura, M. Vestergaard, M. Ishiyama, N. Nagatani, T. Hashiba, E. Tamiya, Development of a novel hand-held toluene gas sensor: Possible use in the prevention and control of sick building syndrome, Meas. J. Int. Meas. Confed. 39 (2006) 490–496. https://doi.org/10.1016/j.measurement.2005.12.014.

[110] J.H. Sohn, M. Atzeni, L. Zeller, G. Pioggia, Characterisation of humidity dependence of a metal oxide semiconductor sensor array using partial least squares, Sensors Actuators, B Chem. 131 (2008) 230–235. https://doi.org/10.1016/j.snb.2007.11.009.

[111] T. Zhang, S. Mubeen, B. Yoo, N. V. Myung, M.A. Deshusses, A gas nanosensor unaffected by humidity, Nanotechnology. 20 (2009). https://doi.org/10.1088/0957-4484/20/25/255501.

[112] H.-R. Kim, A. Haensch, I.-D. Kim, N. Barsan, U. Weimar, J.-H. Lee, The Role of NiO Doping in Reducing the Impact of Humidity on the Performance of SnO2-Based Gas Sensors: Synthesis Strategies, and Phenomenological and Spectroscopic Studies, Adv. Funct. Mater. 21 (2011) 4456–4463. https://doi.org/10.1002/adfm.201101154.

[113] A.D. Clayton, A.M. Schweidtmann, G. Clemens, J.A. Manson, C.J. Taylor, C.G. Niño, T.W. Chamberlain, N. Kapur, A.J. Blacker, A.A. Lapkin, R.A. Bourne, Automated self-optimisation of multi-step reaction and separation processes using machine learning, Chem. Eng. J. 384 (2020) 123340. https://doi.org/10.1016/j.cej.2019.123340.

[114] C.W. Coley, R. Barzilay, T.S. Jaakkola, W.H. Green, K.F. Jensen, Prediction of Organic Reaction Outcomes Using Machine Learning, ACS Cent. Sci. 3 (2017) 434–

443. https://doi.org/10.1021/acscentsci.7b00064.

[115] G.H. Gu, J. Noh, I. Kim, Y. Jung, Machine learning for renewable energy materials, J. Mater. Chem. A. 7 (2019) 17096–17117. https://doi.org/10.1039/c9ta02356a.

[116] W. Sha, Y. Guo, Q. Yuan, S. Tang, X. Zhang, S. Lu, X. Guo, Y.-C. Cao, S. Cheng, Artificial Intelligence to Power the Future of Materials Science and Engineering, Adv. Intell. Syst. 2 (2020) 1900143. https://doi.org/10.1002/aisy.201900143.

[117] Z. Chen, Z. Chen, Z. Song, W. Ye, Z. Fan, Smart gas sensor arrays powered by artificial intelligence, J. Semicond. 40 (2019). https://doi.org/10.1088/1674-4926/40/11/111601.

[118] C. Mendes-Felipe, J. Oliveira, I. Etxebarria, J.L. Vilas-Vilela, S. Lanceros-Mendez, State-of-the-Art and Future Challenges of UV Curable Polymer-Based Smart Materials for Printing Technologies, Adv. Mater. Technol. 4 (2019) 1800618. https://doi.org/10.1002/admt.201800618.

[119] M.E. Karar, A.M. Al-Masaad, O. Reyad, Gasduino-wireless air quality monitoring system using internet of things, Inf. Sci. Lett. 9 (2020) 113–117. https://doi.org/10.18576/isl/090208.

[120] K. Gautam, V. Puri, J.G. Tromp, N.G. Nguyen, C. Van Le, Internet of Things (IoT) and Deep Neural Network-Based Intelligent and Conceptual Model for Smart City, in: 2020: pp. 287–300. https://doi.org/10.1007/978-981-32-9186-7_30.